Naval Information Warfare Center PACIFIC

TECHNICAL REPORT 3303
JANUARY 2023

Ocean Acoustic Analysis of the 1994 Northridge Earthquake

Dr. Scott C. McGirr
Wayne L. Teeter
Dr. Ronald Wroblewski

NIWC Pacific

Naval Information Warfare Center (NIWC) Pacific
San Diego, CA 92152-5001

This page is intentionally blank.

TECHNICAL REPORT 3303
JANUARY 2023

Ocean Acoustic Analysis of the 1994 Northridge Earthquake

Dr. Scott C. McGirr
Wayne L. Teeter
Dr. Ronald Wroblewski

NIWC Pacific

Administrative Notes:

This report was approved through the Release of Scientific and Technical Information (RSTI) process in October 2022 and formally published in the Defense Technical Information Center (DTIC) in January 2023.

NIWC Pacific
San Diego, CA 92152-5001

NIWC Pacific
San Diego, California 92152-5001

A. D. Gainer, CAPT, USN
Commanding Officer

C. A. Jackson
Executive Director (Acting)

ADMINISTRATIVE INFORMATION

The work described in this report was performed by government employees in the Information Operations Division (75600), in the Science and Technology Department (75000), Naval Information Warfare Center (NIWC) Pacific, San Diego, CA.

Released by
Alex Vassil, Division Head
Information Operations Division

Under authority of
Carly Jackson, Department Head
Science and Technology Department

ACKNOWLEDGMENTS

Two New Professionals (NPs) at NIWC Pacific worked on this effort for three-month tours. The Office of Naval Research (ONR) Naval Research Enterprise Intern Program (NREIP) provided summer internships at NIWC Pacific for six students for 10-week tours. Two interns of the NAVSEA internship program assisted during three-month tours at NIWC Pacific. The NIWC Pacific Technical Library & Archives (84310) provided help with identifying and obtaining relevant material (literature and maps). Essential assistance was provided by Lawrence Livermore National Laboratory (LLNL) with both data recording and storage.

Editor: MRM

EXECUTIVE SUMMARY

Ocean acoustic activity was analyzed before and after the 1994 Northridge earthquake. Hydrophones in the California Continental Borderland recorded primary waves (P-wave) and tertiary waves (T-wave) over an 80-hour period. P-waves near 0 to 15 Hz and T-waves 5 to 20 Hz were differentiated using spectrograms. Ocean-based acoustic data was analyzed and compared to concurrent land-based seismographic data. The P-waves detected correlated with the land seismic events. The T-waves detected did not correlate with seismic data. T-waves, localized by Line of Bearing (LOB) cross-fixing, were along the Ferrelo Fault zone in a major lateral offset. Land seismic sensors showed no precursors to the earthquake. Ocean acoustic sensors showed seaquakes occurring at a rate of 5.3/hour, which stopped 31 hours 20 minutes prior to the main earthquake and returned to near prior activity levels 16 hours later. Ocean quakes may indicate energy release during earth movement and its absence indicates energy accumulation as elastic strain in rocks. Hydrophones provide a valuable means to monitor geologic activity in borderland regions and can contribute to the understanding of coastal earthquakes.

OBJECTIVE

The objective of this research was to determine if there are changes in ocean acoustic activity preceding the 1994 Northridge earthquake. This study relied on data fusion, analyzing both ocean acoustic and land seismic data. Hydrophones have been shown to be more than an order of magnitude more sensitive than land-based seismic sensors for earthquake detection in coastal regions (Fox, 1994). Changes in acoustic activity has been found with volcano eruptions (Fischer, 1994; Chouet, 1996).

METHODS

Ocean acoustic data was acquired for 80 hours from 14 January 1994 at 20:12 through 18 January 1994 at 03:30 GMT. The data was obtained from hydrophones in the Southern California Continental Borderland. Land seismographic data was obtained over the same period of time online from the Southern California Earthquake Data Center (SCEDC). Seismic data was from latitude 31 to 36 N and longitude 124 to 115 W. Earthquakes have been shown to give rise to P-waves (Primary), S-waves (Secondary or Shear) and T-waves (Tertiary). Hydrophone recording were 2 Hz to 100-Hz. Noise of biologics and shipping was reduced by low pass filtering below 30-Hz. Acoustic pressure waves were characterized by detection time, duration, peak amplitude and prior noise level. The sensor pressure (Lp) was used to determine intensity (Li), aka local field power.

Of interest was determination of source power and equivalent magnitude. Determination of source power requires knowledge of source location. This was determined differently for P- and T-waves. P-wave origins were localized by correlation with seismic data and quantified by modeling seismic events traveling through land. T-wave origins were localized by LOB cross-fixing and quantified by modeling sound travel through water. The source level power (W/s) was estimated by modeling sound travel through media to sensors (W/m^2). This was done in two ways: 1) modeling the area of power dissipation (Power= Area*Intensity); and 2) for T-waves the Bellhop model was also used for determination of Source Level (SL) from Receiver Level (RL) and Transmission Loss (SL= RL+TL). Note that noise was previously removed from pressure and derived intensity (i.e. RL).

Source power was converted to equivalent seismic magnitude local (M_L) that is most commonly used for quantifying earthquakes. The P-wave source power at origins were correlated to seismic quakes in Northridge, CA, and regression analysis was used to derive a formula to determine seismic magnitude. Land seismic sensors did not detect any of the seaquakes found by hydrophones. Thus, converting T-wave source power to seismic magnitude required other means. The means used was to rely on power to magnitude formula found in the analysis of 1992 Cape Mendocino seaquake (Dziak, 1997). In addition, the conversion formula found with P-waves analysis was reviewed.

The graphics used for Figures 1, 9 and 10 were made with GeoMapApp tools of Columbia University. The graphics can be reproduced from data in Appendix. In addition, the tools were used for determining ocean bottom profiles used for Bellhop propagation modeling. Sample output and data tables are given in the appendix.

CONCLUSIONS AND RECOMMENDATIONS

Hydrophones recorded acoustic activity in Southern California Borderland associated with the 1994 Northridge earthquake. Acoustic T-waves occurred regularly, stopped 31 hours and 20 minutes prior to the 1994 Northridge earthquake, and then resumed. The land quakes recorded on seismic networks were detected as P-waves. The ocean quakes recorded as T-waves were localized to the Tanner basin, along with the Ferrelo Fault zone and Lateral Offset. This study found present day quake or venting activity in this specific area previously not reported. Duration of the sound signals were of value estimating earthquake magnitude for P-waves but not T-waves. An equation was developed relating P-wave sound power (Lw) to seismic magnitude (M_L). The timeline for activity over the 80 hours is consistent with tectonic plate theory showing stress buildup and release in form of earthquakes. Further study of the Southern California Borderland could prove valuable for developing forecasting models of future earthquakes and seismic activities.

ACRONYMS

AD	Analog-to-Digital (acoustic unit conversion)
DBFS	Decibels Below Full Scale
BOEM	Bureau of Ocean Energy Management
CSLC	California State Land Commission
GMRT	Global Multi-Resolution Topography
GMT	Greenwich Mean Time
LOB	Line-of-Bearing
Li	Log intensity (local) dB rel reference watts/m^2
Lp	Log pressure (local) dB rel reference uPa/m^2
Lw	Log power (source) dB rel reference watt
M_D	Magnitude Duration (in seconds)
M_L	Magnitude Local (Richter scale)
M_O	Seismic Moment dB N-m (Newton-meters)
M_w	Magnitude Moment
NAVSEA	Naval Sea Systems Command
NEIC	National Earthquake Information Center
NIWC Pacific	Naval Information Warfare Center Pacific
NREIP	Naval Research Enterprise Intern Program
NUWC	Naval Undersea Warfare Center
NSWC	Naval Surface Warfare Center
ONR	Office of Naval Research
RMS	Root Mean Square
RVS	Receiving Voltage Sensitivity
SCEDC	Southern California Earthquake Data Center
SCSN	Southern California Seismic Network
SOFAR	Sound Fixing and Ranging (channel)
USGS	United States Geological Survey

This page is intentionally blank.

CONTENTS

APPENDICES

FIGURES

TABLES

This page is intentionally blank.

1. INTRODUCTION

1.1 PURPOSE

The purpose of this research was to determine if there are changes in ocean acoustic activity associated with coastal earthquakes. Previous studies have shown rock stress can induce changes in earth's electric and magnetic fields that can explain observed lights and other phenomena prior to earthquakes (Freund, 2010). Acoustic emissions have preceded coal-mine collapses and volcano eruptions. Sound emissions (250 to 1,250 Hz) caused from rock cracking 15 to 30 hours prior to rock-burst have been used to warn of mine failures and suggested for indicating earthquakes (Armstrong, 1969). Changes in long-period seismic activity and sulfur dioxide gas emissions have preceded ocean volcano eruptions (Fischer, 1994; Chouet, 1996). Volcano tectonic events, caused by rock cracking, are evident as P- and S-waves.

1.1.1 Objectives

The objective of this research was to determine if there are changes in ocean acoustic activity preceding the 1994 Northridge earthquake. This study relied on data fusion, analyzing both ocean acoustic and land seismic data. Hydrophones have been shown to be more than an order of magnitude more sensitive than land-based seismic sensors for earthquake detection in coastal regions (Fox, 1994). Changes in acoustic activity has been found with volcano eruptions (Fischer, 1994; Chouet, 1996).

1.2 BACKGROUND

Ocean-based acoustic sensors have been used to study ocean explosions, volcanic eruptions, and hydrothermal venting (Hammond, 1991). Acoustic sensors have been found to be more sensitive than seismic sensors for detection of ocean tremors (Fox, 1994) and are effective for event localization (Stephen, 2013). The frequency of seismic energy is low, ranging from near 0 Hz to more than 20 Hz (the lower limit of the human audible range). Hydrophones can distinguish three seismic energy phases or waves named in accordance with observed transmission speeds through water. Primary waves (P-waves) are caused by longitudinal compression forces and can travel through both solids and liquids. Secondary waves (S-waves) are caused by transverse shearing forces and can travel only through elastic rock. S-Waves can be observed indirectly by hydrophones when vertical motion is converted to acoustic energy near bottom-mounted sensors (Blackman, 2000). Tertiary waves (T-waves) are caused by the release of sound energy into water. These waves are rapidly attenuated in land but can travel long distances in water through the Sound Fixing and Ranging (SOFAR) channel. T-wave acoustic and seismic signal strengths have been correlated (Dziak, 1997).

1.2.1 Regional Setting

Coastal areas surrounding the Pacific basin contain seismically active belts known as the Ring of Fire. Within the basin, there is relative calm, with the exception of a few island groups such as Hawaii. Sources of T-waves have been traced to these seismically active areas and to deep offshore trenches (Johnson, 1966). This study took place along the coast and off-shore ocean region known as the Southern California Continental Borderland that is an active undersea landscape extending 200 km offshore. It is bounded seaward by a Pacific Plate moving northwest and landward by the North America plate moving southeast. Coastal geography plays an important role in seismic-acoustic energy conversion on the seafloor. T-waves may represent the release of energy originating below the ocean floor or from adjacent coastal regions.

For continental borderland earthquakes, T-waves can be modeled accurately as individual point sources distributed uniformly over the ocean floor (Groot-Hedlin, 1999). Simulation studies indicate that T-waves are excited most efficiently in shallow water within a few hundred kilometers (km) of an earthquake epicenter. However, steep land-ocean interfaces allow better penetration of energy into the ocean than shallow interfaces (Okal, 2007). Empirical studies have shown that many small seismic events produce P- and S-waves but not T-waves (Blackman, 2000).

The 1994 Northridge earthquake occurred at 12:31 (GMT) on 17 January and had a moment magnitude of 6.7 (SCEDC Catalog). Moment magnitudes (M_w) are roughly equivalent to local magnitudes (M_L) on the Richter Scale (Kanamori, 1977; and Baruah, 2012). $M_w = 2/3 \, Log_{10} M_O - 6.03$ where M_O is seismic moment in N-m^2 equal to rigidity*area*slip. Seismic signal duration has a relationship to both M_w and M_L. Magnitude duration (M_D)$= C_0 + C_1 \, Ln \, D_S + C_2 \, D + C_3 \, h$ where D_S is duration in seconds, D is distance in km, h focal depth in km and the Cs are empirical constants (Lee, 1981). A comparison of 162 earthquakes in India and in other studies show similar M_W, M_L and M_D values within .1 or .2 magnitude units (Bora, 2016).

The hypocenter was located 118.54 W longitude 34.21 N latitude, at a depth of 18.4 km. The epicenter (on surface) was located 32 km northwest of Los Angeles at a distance of about 35 km from the coastline. The rupture occurred along the Northridge thrust fault (also known as the Pico thrust) and had a rupture area of 300 sq km. Shocks were observed over a surface distance of 31 km. This earthquake was selected for this study because it occurred in proximity to two underwater research acoustic arrays recording at the time. As shown in Figure 1, this is a region of northwest running faults associated with the San Andreas Fault and off shore faults. The location of the earthquakes M>5.0 from 1973 to 2013 recorded by USGS-NEIC are depicted as circles with size reflecting magnitude and color depth. The graphic was made with GeoMapApp tools courtesy of Columbia University.

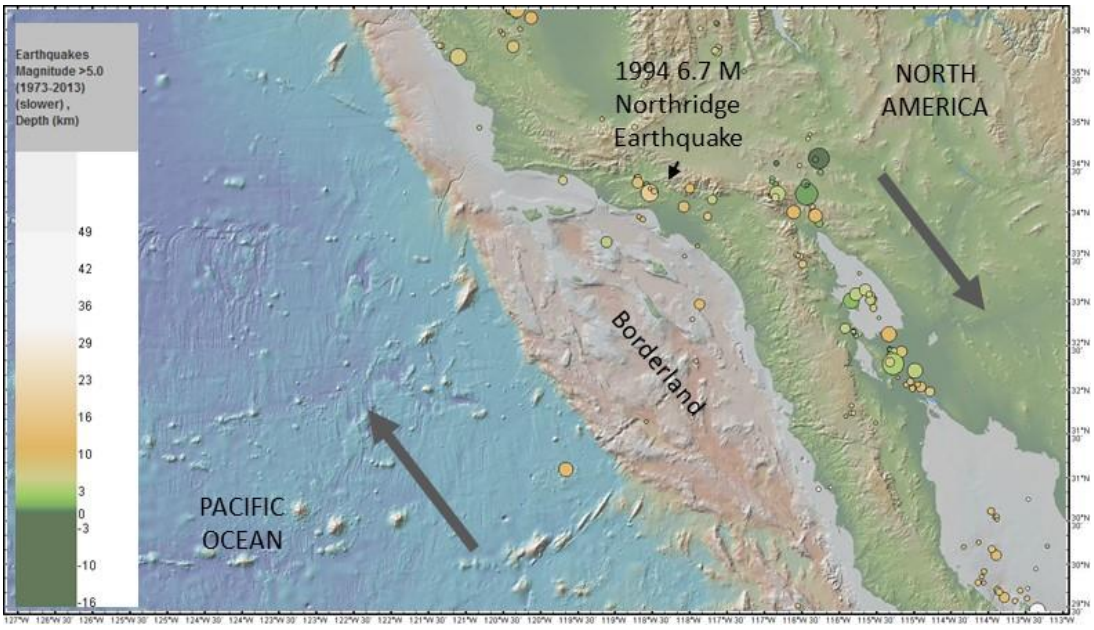

Figure 1. Map of Southern California Borderland.

2. METHODS AND MATERIALS

2.1 METHODS

Two horizon acoustic arrays, located on the seabed, collected the acoustic data used for analysis. A 30-Hz, low-pass filter was used to reduce noise and unwanted signals such as Finback whales. A single phone on the South array was used for detailed analysis. Hydrophone analog-to-digital (AD) conversion provided ±32,768 discrete sound levels, 15-bit measurement with 1-bit for +/- sign (90.3 dB dynamic range). Noise was measured for a few minutes prior to signals. Pressure waves detected above noise were recorded as discrete 'events'; primary signal parameters measured were time, duration (seconds), peak amplitude in AD count. Isolated signal spikes were discarded. In addition, total pressure for events was recorded that could be used for energy calculations.

The total 80 hours were analyzed in 2-hour time intervals. Amplitude was direct measure of AD units and integration tools used Root Mean Square (RMS). As shown in Figure 2, data was both viewed as phone amplitude (A) and frequency spectrograms (B) to characterize signals. Signals above noise were recorded as events. Peak values were used for pressure amplitude. A 60-minute period is shown of (A) hydrophone amplitude in AD units, and corresponding (B) frequency spectrogram. P-waves (0 to 15 Hz) and two T-waves (5 to 20 Hz) can be differentiated by pulse shape, frequency, and speed of travel. P-wave pulses are typically sharper and amplitude of both types of waves trail off at higher frequencies. No S-wave were evident in this study.

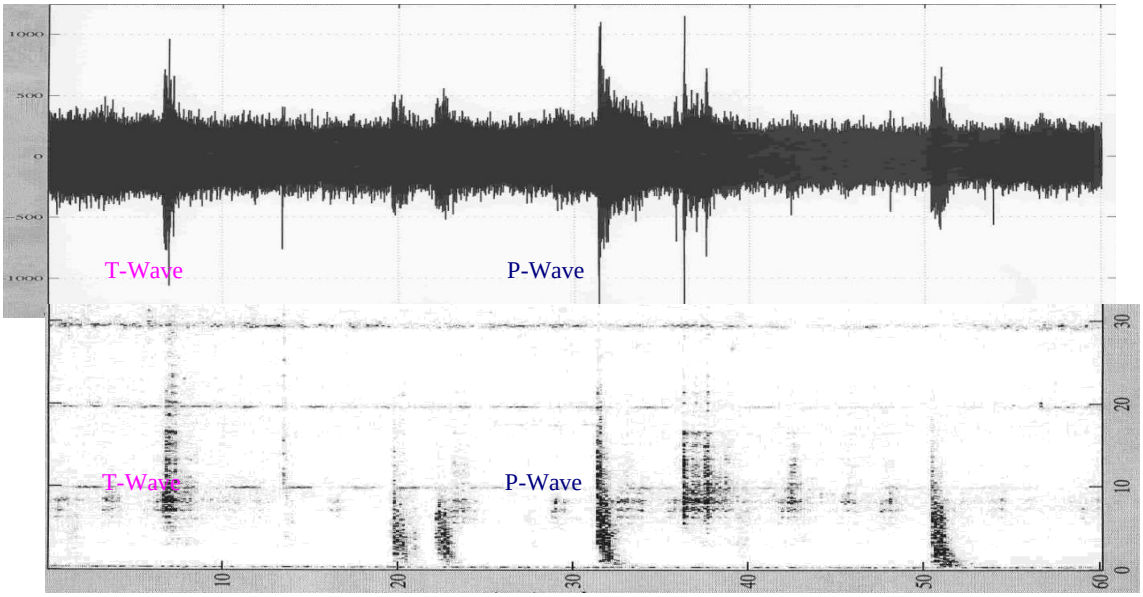

Figure 2. Recorded data A) phone and B) spectrogram

2.1.1 Study Design

Acoustic wave amplitude, recorded as AD units were converted to Log pressure (Lp). Calculation methods used were consistent with those described by NSWC (Butler, 2018). Generic hydrophone values were used for Resolution (R), Gain (G) and Sensitivity (S). Hydrophone sensitivity is a ratio of voltage to pressure, specific to the sensor, and referred to as Receiving Voltage Sensitivity (RVS). This is over an acoustic frequency range. Resolution is the voltage of 1 AD unit in micropascals (uPa). Voltage is the product of AD count and resolution, V= 20Log(AD count*voltage/count). Log pressure in dB re uPa is Lp = V + R + G – S. This study used seawater parameters.

2.1.1.1 Hydrophone Measures

Measures for field power (aka intensity) used for this study are shown in Table 1. Corresponding values are shown for three media. The study used seawater parameters. The hydrophones at the ocean bottom receive seismic energy transfer via land and are converted in the water column for sensor recording. Log values do not have units but are expressed as dB relative to the medium standard. Different values exist for media and references vary according to standards. The log pressure (Lp) and log intensity (Li) have similar numbers but are different measurements and associated units. The difference of minimum to maximum values reflects the sensors' dynamic range.

Table 1. Acoustic field power.

Value	Air	Sea	Land	Units	Description
po	2E-05	1E-06	1E-06	Pascal	Reference Pressure
d	1.29	1023.6	2950	Kg/m^3	Density of media
c	343	1,500	7250	meters/s	Speed of sound
dc	411.6	1.5E+6	2E+07	$Kg/m^2/s$	Impedance, z=dc
Io	1E-12	6.7E-19	4.7E-20	W/m^2	Intensity, i= $(p^2)/dc$
Min Lp	5.30	31.32	31.32	dB re po	Log Pressure
Max Lp	95.6	121.6	121.6	dB re po	Lp=20Log(p/po) dB
Min Li	5.18	31.20	31.32	dB re po	Log Intensity
Max Li	95.5	121.5	121.6	dB re po	Li= 10Log(i/io) dB

2.1.1.2 Acoustic Source Models

Measures for source power used for this study are shown in Table 2. Source power calculation requires knowledge of the origin of source. The earthquake origin is not explicitly known and for this study was determined by correlation to seismic data for P-Waves and array LOB cross fixing for T-Waves. Calculation of source power also requires knowledge of transmission loss in travel to sensor. Transmission loss in this study was modeled in two ways. The first method was modeling area enclosing source to sensor and converting local intensity measured at sensor to that at originating source. This assumes uniform wave power dissipation at boundary of area. The equation is Power= Area*Intensity. This study modeled area as a cylinder with radius equivalent to horizontal range and height the vertical depth of transfer media reflecting boundaries. The second method was modeling the sound travel through water from source to sensor to determine path loss and source power. The Source Level (SL) equals Receiver Level (RL) plus the Transmission Level (TL).

The acoustic energy can be determined by integrating the wave power at source over duration, or LogE= Lw(avg)+Log(time) in Watts. For this study it was estimated using E= 0.5*peak source power (watts) * time (seconds) in Joules. The seismic energy estimate used was LogE= 1.44 M_L +5.24 (Bath 1966). Alternate energy estimates exist for magnitude (local) of LogE= 1.5 M_L + 4.8 in Joules (Gutenberg, 1956) and LogE= 1.5M + 4.4 in Joules (Choy, 1995). A more accurate means for determination can be made from moment magnitude (Mw) if area of rupture and displacement are known (Aki, 1967). However, this is often not known and magnitude local was used.

Table 2. Acoustic source power.

Measure	Equation	Units	Description
Peak Pressure	Lp=20Log(p/po) dB	dB re uPa	Acoustic waves
Intensity dB	Li= 10Log(i/io)	dB re W/m^2	Field power (local)
Power 1	Power= Area*Intensity	Watts/s	Source power (PL)
Power 1 dB	Lw= 10Log(As/Ao) + Li	dB re W/s	Area dissipation
Power 2	Source Level	dB re W/s	Source Level (SL)
Power 2 dB	SL= RL + TL	dB re W/s	Path dissipation
Magnitude*	M_L = .031*Lw – 3.30	M_L	Power (Lw) via T-Wave
Magnitude**	M_L = .0567*Lw – 7.8221	M_L	Power (Lw) via P-Wave
Energy	LogE= Lw(avg) + Log(s)	Watts	Acoustic measure
Energy***	LogE= 1.44 M_L + 5.24	Joules	Seismic measure

* Dziak (1997), ** determined in this study, *** Bath (1966)

2.2 MATERIALS

Ocean acoustic data were acquired for 80 hours from 14 January 1994 at 20:12 through 18 January 1994 at 03:30 GMT (Greenwich Mean Time). Data resided on two Exabyte tapes and had been high-pass filtered 3 dB down at 2 Hz, and rolled off steeply after that. The data were sampled at 200 Hz and stored as 16-bit integers. The sampling rate provided an effective spectral analysis for frequencies at 2 to 100 Hz. Single phone data was analyzed manually using Adobe Audition and multiple phone array data processed using MATLAB® signal processing tool kit. The array processing was performed for event localization of T-waves. The power measures are in this study are peak amplitudes W/s and dB consistent with seismic magnitudes. The mid-array locations on the seabed were used for calculations. The S. Array depth averaged 1075 meters.

Land seismographic data was obtained online from the Southern California Earthquake Data Center (SCEDC). The Southern California Seismic Network (SCSN) has collected data for over 90 years and information is available (Hutton, 2010). Seismic data analyzed was from latitude 31 to 36 N and longitude 124 to 115 W. The data consists of different magnitude types that were used without adjustments. Recorded events were primarily M_L (Richter scale). The sensitivity known as magnitude completeness was M_L ~ 1.8. Duplicate records were removed as well as man-made events such as quarry blasts. This was thus assumed “ground truth” for earthquake time, location, magnitude, and duration. Both seismic and acoustic sensors used the GPS for time. The accuracy of acoustic time stamps of recorded files was 0.1 seconds.

This page is intentionally blank.

3. RESULTS

3.1 RESULTS

Seismic-acoustic activity of the 1994 Northridge earthquake was studied. Of particular interest was relationships of activity at sea and on land. This earthquake was not associated with major faults. This is consistent with previous findings for this region of Southern California where a general lack of association has been found between minor shocks and major faults (Gutenberg, 1956). Small shocks have been found to cluster near minor faults that are numerous in this region. S-waves do not travel as far as P-waves and were not observed in this study. Similarly, P-waves were present and S-waves absent in studies of the 1992 Cape Mendocino earthquake when acoustic sensors were located about 400 km from seismic events (Dziak, 1997).

3.1.1 Key Findings

A comparison was made of quakes detected by seismic land sensors and those by acoustic ocean sensors over an 80-hour time period. Seismic and acoustic sensors detected quakes before and after the 1994 Northridge earthquake. These sensors can be compared by plotting seismic magnitude (M_L) and acoustic amplitude (Lp) of quakes detected. As shown in Figure 3A, the seismic-detected quakes' rate of occurrence did not vary before the main shock. These quakes were on land. As shown in Figure 3B, the acoustic-detected quakes varied significantly prior to the main shock. These quakes were at sea. To clarify signal types, acoustic signals identified as T-waves are colored cyan and those identified as P-waves blue. Properties are discussed in methods. Seismic signals are colored a darker blue and, as discussed later, are similar to acoustic P-waves. Of great interest is the fact that acoustic ocean sensors showed change in rate of quake activity prior to the 1994 earthquake.

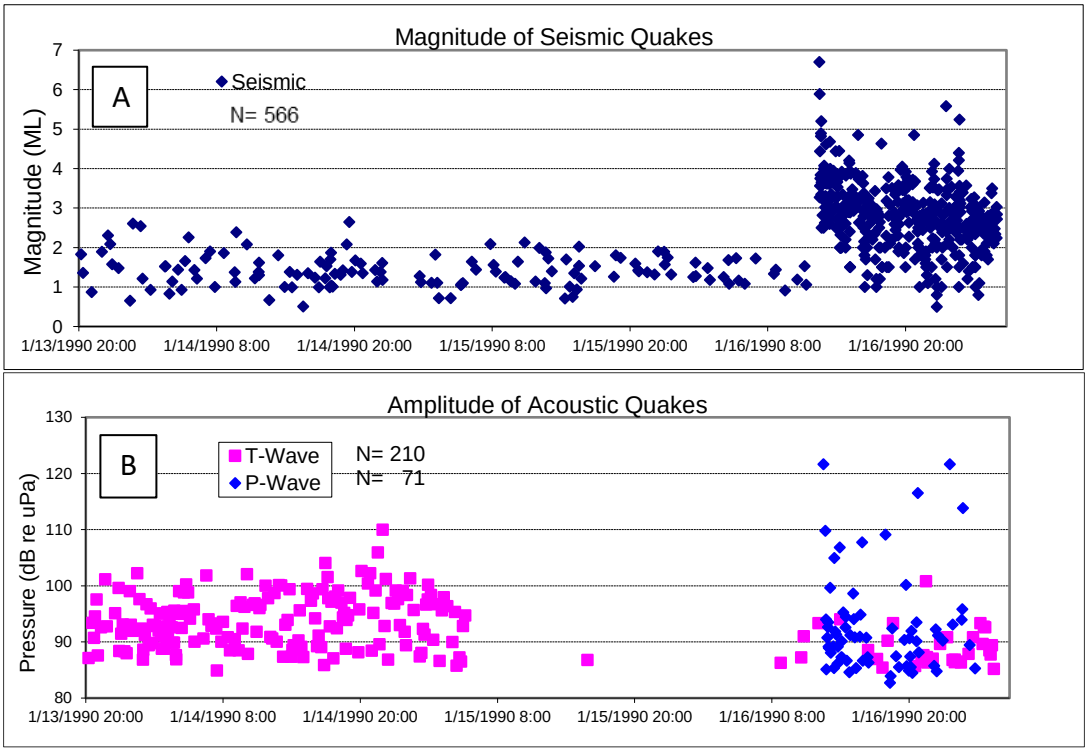

Figure 3. Quake detections A) seismic and B) acoustic.

To determine if seismic and acoustic events sequences occurred randomly, comparisons were made of the observed data to that expected for rate of occurrence under a random Poisson process. The number of seismic and acoustic events in 2-hour time periods prior to the earthquake fit random Poisson distributions. Thus, the acoustic data appeared to arrive randomly at a relatively constant rate for the first 33-hours as did the seismic data in the first 47.9-hours. For this initial period, 5.3 quakes per hour were detected acoustically. There was 14 samples of 2 hours and 17 quakes with Chi-Square value of 21, and P=.05. However, for the later periods the occurrence of quakes during the 2-hour samples did not fit Poisson distributions. As evident in Figure 3B, after the rate of occurrence changed, the data no longer fit a random Poisson process. Of particular interest is the quiet T-wave period of 31.3-hours prior to the 1994 Northridge earthquake.

3.1.1.1 Seismic Sensors

A summary of land seismic data is shown in Table 3. The absence of seismic precursors is apparent and consistent with previous findings (Kedar, 1996). Increases in both magnitude and rate of occurrence occurred after the main shock. The average depth of quakes decreased from 6.4 km before to 5.4 km after the main earthquake. Very little correlation was found between the magnitude and depth of quakes. A total of 136 shocks were observed over a 64.5-hour period prior to the Northridge earthquake and 431 shocks over a 15.5-hour period after the earthquake. Seismic quake activity occurred at an average rate of 2.3 events/hour prior to the earthquake and decreased afterwards consistent with decay laws. Several decay laws exist (Gasperini, 2009).

Table 3. Seismic detections over 80-hour study.

Seismic	Before Main Shock	After Main Shock
Start Date-Time	94/01/14 20:00	94/01/17 12:30
End Date-Time	94/01/17 12:30	94/01/18 4:00
Interval (hours)	64.52	15.48
Detections	136	431
Type	Seismic (M_L)	Seismic (M_L)
Avg Magnitude	1.82	4.26
Avg Depth (km)	7.26	5.94

3.1.1.2 Acoustic Sensors

A summary of ocean acoustic data is shown in Table 4. T-wave detections did not show average change in peak pressure amplitude before or after the earthquake but did show changes in rate of occurrence. There were three activity periods: (1) baseline rate of 5.3 per hour, (2) rate decrease to only 0.16/hour (quiet acoustic period); and (3) after the Northridge earthquake an increasing rate with average of 2.01/hour over the remaining period. No P-waves were observed before the earthquake but after it, there was a rate of 4.90/hour (decreasing). T-wave rate of occurrence remained fairly constant for 33 hours, stopped abruptly at 31 hours and 20 minutes prior to the earthquake, and then resumed activity after the earthquake (increasing). P-waves appeared at the time of the earthquake and tapered off over a period of 16 hours. Peak pressure was measured above the background noise in AD units prior to dB conversion to maintain units (dB re uPa).

Table 4. Acoustic detections over 80-hour study.

Acoustic	Before Main Shock		After Main Shock	
Start Date-Time	94/01/14 20:12	94/01/16 05:11	94/01/17 12:31	94/01/17 12:31
End Date-Time	94/01/16 05:11	94/01/17 12:31	94/01/18 03:25	94/01/18 03:25
Interval (hours)	64.52	15.48	14.9	14.9
Detections	175	5	30	71
Type wave	T-Wave	T-Wave	T-Wave	P-Wave
Avg Peak P (Lp)	92.69	87.38	87.44	91.14
Avg Noise (Ln)	74.23	71.91	73.21	73.21
Avg Duration (s)	112.88	98.80	48.13	77.87

3.2 STATISTICAL ANALYSIS

3.2.1 Acoustic Properties

The acoustic detections behaved as expected for earthquakes. As shown in Figure 4, the number of events decreased with quake size increase when measured by either peak pressure amplitude (Lp) or duration(s). For the geographic area and time period of this study, 210 T-waves and 71 P-waves were recorded. The ocean area of Southern California Borderland and surrounding land are seismically active. The average acoustic noise level was 73.8 dB re uPA, which is within the range reported in previous studies for this area (McDonald, 2008; Urich, 1984). The average signal peak pressure was 92.9 dB re uPa and Signal to Noise Ratio (SNR) of 19.4. The relation found was log-linear with some drop off due to small quake-detectability limits. The lowest amplitude quake detected was 82.7 dB re uPa and shortest duration quake detected was 10 seconds.

3.2.2 Acoustic Distributions

Properties of acoustic signals were analyzed. The 210 T-waves recorded had mean pressure Lp= 91.82 dB re uPa and range of 82.03 to 109.81. The mean duration was D= 103.3 seconds and ranged from 10 to 321 s. The 71 P-waves recorded had mean pressure Lp= 91.14 dB re uPa and ranged from 78.63 to 121.60 (saturation). The mean duration was D= 77.87 seconds and ranged from 16 to 523. As shown in Figure 4A, the peak pressure distributions of both T- and P-waves are skewed with decreasing occurrence of larger size quakes as expected. Figure 4B, shows the relation of quake event duration to amplitude pressure. T-waves had greater variability. The linear regression calculated for P-waves showed a higher regression coefficient than T-waves.

All earthquakes arise at hypocenters under-ground but seaquakes can be detected at epicenters on surface over land at ocean bottom. These results are consistent with the fact that P-waves travel through a relatively homogeneous rock media and T-waves travel through water that has variation in paths. Volcanic seismicity has been shown to introduce greater numbers of small events (Fox, 1994). While active volcanic activity has not been reported in the area of study, the bedrock does have Miocene volcanic rock (Legg, 2015). T-waves may have a non-direct path through a land-ocean boundary, bottom and surface scattering, and possible bathymetric radiators (Williams, 2006). P and T-wave origins and paths traveled is important for acoustic characterization of quakes.

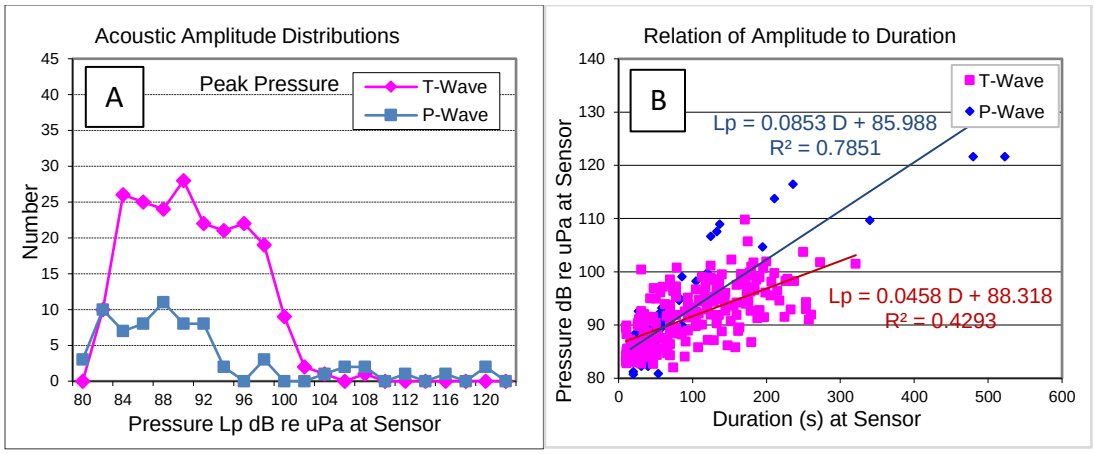

Figure 4. Acoustic A) distributions and B) regression analysis.

Earthquake strength can be measured by acoustic pressure and duration. Past studies have shown a relationship between acoustic amplitude and duration (Okal, 1986 and Okal, 2007). Seismic waves consist of both longitude and shear waves denoted as P and S. The shear waves produce the most damage. A good review of seismic process measures is given by Bath (Bath, 1966). In this study, correlations of the pressure amplitude to duration, recorded at sensor, were higher for P-waves than T-waves. As discussed later, duration was found to be a more reliable measure of earthquake size for P-waves than T-waves. The regression analysis results are as follows:

T-wave:	Lp = 0.0458 D + 88.318	R^2= .43	(1)
P-wave:	Lp = 0.0853 D + 85.988	R^2= .79	(2)

3.2.3 Earthquake Magnitude

It was desired to find quake seismic magnitude M_L (Richter scale) for acoustic detections. This is a peak measure value on seismograph. Peak acoustic pressure was used in this study to maintain consistency. A number of differing seismic magnitudes scales exist and a review is given by Bath (Bath, 1966). Magnitude local (M_L) was in the SCEDC data set used for this study. It is also more commonly used for earthquake size characterization. To determine earthquake seismic magnitude from hydrophones, acoustic source power was converted to the magnitude.

It is important to relate underwater acoustic measures to seismic parameters. All hydrophone recordings are at a distance from the earthquake. Source power determination requires modeling sound wave travel to sensor and inferring the power loss. Source power can then be converted to seismic magnitude using empirical data. This is based on regression analysis of earthquakes with acoustic and seismic readings. The general steps of this study are as follows:

1) calculate sensor pressure from analog digital count and instrumentation.

2) calculate intensity given media density (d) and sound speed (c), i= p^2/dc.

3) determine sound origin from multiple acoustic sensors or by other means

4) model sound dissipation from source to sensor by area model or ray trace

5) convert acoustic source power, Lw, to equivalent seismic magnitude, M_L

6) summarize acoustic and seismic energy and power changes in 80-hr data

3.2.4 P-wave analysis

A comparison was made of seismic and acoustic data to determine if quakes in the Northridge, CA area gave rise to the acoustic sensor detections. Because it was anticipated that arrival of energy at the sensors would differ for P- and T-waves due to different propagation speeds and paths, comparisons with seismic events were made using sliding time windows. For the 71 P-waves observed, a high correlation with seismic events (> M_L 3.1) was found for time lags of about 32 seconds. For the source-to-sensor distances, this resulted in an average propagation speed of 7.25 km/s with a standard deviation of 0.45. This speed is consistent with P-wave speeds found in this region of 5.3 to 8 km/s (Dziak, 1997; Hauksson, 2000; Lin, 2007; Nishimura, 1989; Slack, 1999). Although the depth of the quake origins varied from 0 to 23 km, no differences were found in propagation speed due to depth. With a water sound speed of 1.5 km/s, a time delay of over 2-minutes would be expected for T-waves emanating from coastal regions. In this study, land seismic events were not found to give rise to ocean T-waves. The inland distances of the seismic events from the coastline ranged from 5 to 35 km. It is likely that distances were too great or bottom topology did not support seismic-to-acoustic energy conversion for generation of T-waves. However, the P-waves showed agreement in time of arrival and size with seismic events recorded on the SCSN.

3.2.4.1 P-wave origins

P-waves were correlated to seismic recordings. There is loss of signal strength from the origin to sensor. The loss is primarily due to spreading and attenuation in medium with distance. Some signals not detected may have occurred within bounds of preceding signals preventing detection, or fell below the threshold used for signal declaration. The acoustic saturation level is equivalent to M_L 6.04 and was reached with the main shock and the largest aftershock. The pressure amplitude of P-waves and magnitude of seismic events exhibit a linear relationship (Figure 5A). The acoustic signal duration shows a similar linear relationship (Figure 5B). These measurements of P-waves at sensor do not account for loss of energy but still have relatively high correlations.

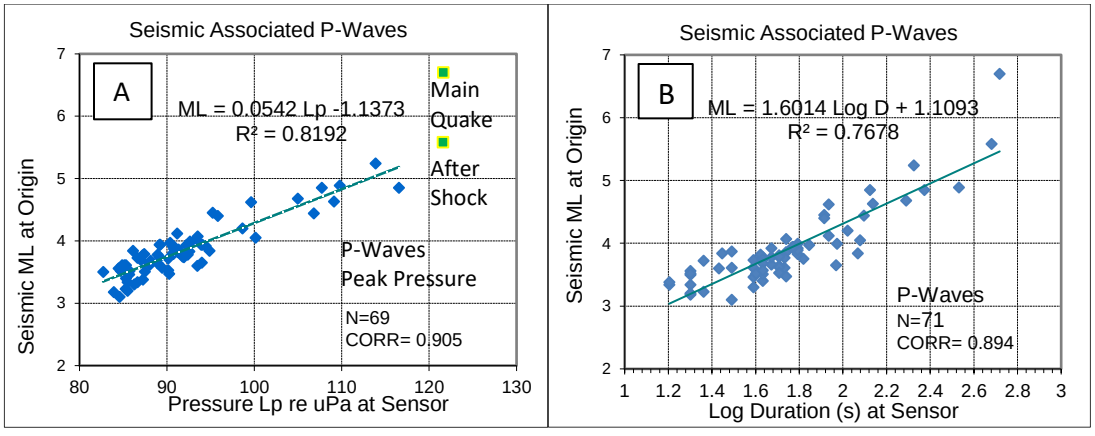

Figure 5. P-wave analyses: A) pressure and B) duration.

This enabled the use of seismic data to established the magnitude of P-waves. A log-linear, least-squares fit yields equations for seismic and acoustic sensor detections of the same events, as follows:

P-waves (pressure): $M_L = 0.054\ Lp + 1.137$ $R^2=.82$ (3)

P-waves (duration): $M_L = 1.601\ LogD + 1.109$ $R^2=.77$ (4)

3.2.4.2 P-wave magnitudes

The analysis results are shown for P-waves in Figure 6. Shown in Figure 6A, all 71 P-waves were correlated to seismic locations, consistent with travel times. The source power was determined from local intensity by modeling the area as a cylinder with radius equal to range from sensor to quake origin and height equal to depth of crust from surface to mantle. A height of 24 km is based on a vertical ground profile of Borderland area (ten Brink, 2000: see Line 2). The local intensity at sensor of 1 m^2 area was increased by cylinder area to estimate source power. Shown in Figure 6B, is a regression analysis of the resulting acoustic source power estimates to quake magnitudes.

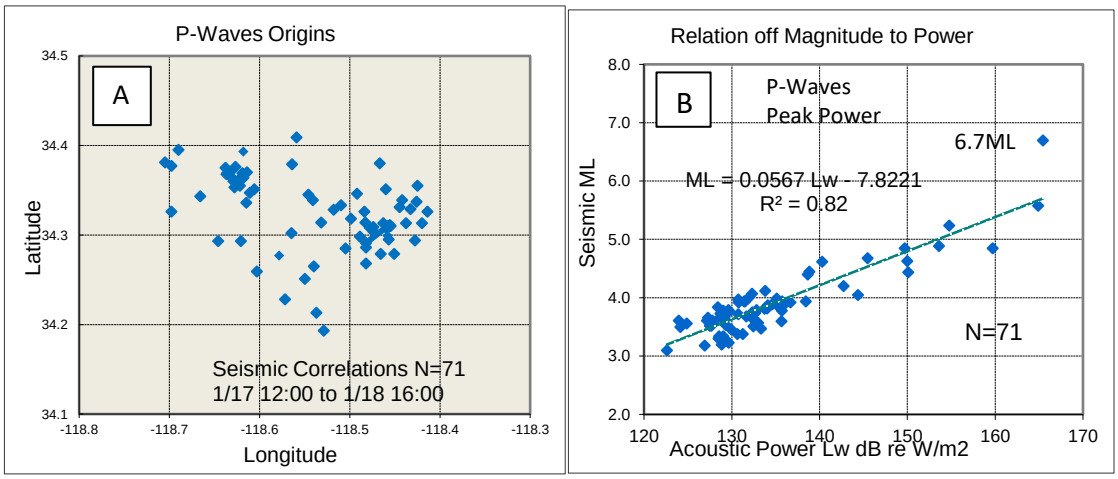

Figure 6. P-waves: A) land origins and B) regression analysis.

The correlation of signal transmission strengths is consistent with previous studies (Dziak, 1997; Ito, 2012). The transmission paths of P- and T-waves, from land (continental) and oceanic origins influences signal amplitude and duration. The relationship of seismic magnitude to acoustic duration is valuable for two reasons. First, duration can avoid problems of sensor amplitude saturation, and second, signal duration may prove more resistant to attenuation with distance. The regression equations can be used to convert acoustic source to seismic magnitude M_L. While equation (5) below relied on modeling sound power (Lw) dissipation, equation (6) only used sound duration (D) in seconds at sensor with expectation of little travel loss. These are of value for P-Waves.

P-waves (dissipation): $M_L = 0.0567\ Lw - 7.8221$ $R^2=.82$ (5)

P-waves (duration): $M_L = 1.601\ Log\ D + 1.109$ $R^2=.77$ (6)

3.2.5 T-wave analysis

T-wave analysis varied from that of P-waves in two important ways. First, P-wave origins were determined by correlation to seismic origins. This was not possible for T-waves as no correlations with land seismic data was found. Thus, for T-waves two hydrophone arrays were used to locate the

origins. Second, P-waves could use seismic data to determine the magnitude of quakes based on existing sensor networks that are very accurate (SCSN). However, for T-waves no matching seismic recordings were available. To determine the magnitude of quakes detected by T-waves other means are needed. This can be done by determining power and converting to magnitude using a prior study (Dziak, 1997) or calculating signal energy or maximum amplitude and converting to magnitude (Ito, 2012). T-Wave duration was found not to correlate well to magnitude (Ito, 2012). For this study, P-wave magnitude conversion of source power (Lw) to magnitude (M_L) was found but for T-Waves its accuracy is not verifiable.

3.2.5.1 T-wave origins

T-wave origins were determined by Line-of-bearing (LOB) cross fixing using two acoustic arrays, designated North and South. The T-waves had 127 LOBs detected at the South array and 27 at the North array. Figure 7A shows the 27 quakes localized by cross fixing the two arrays. The localized quakes are in the Borderland of Southern California.

3.2.5.2 T-wave magnitudes

T-wave magnitudes were estimated from acoustic source power (Lw). The source power was determined using two different models. The first model used was power level (PL) equal to area encompassing the source multiplied by intensity: PL= A*I. It is assumed local intensity is 1 m^2. This is normally converted to log scale and expressed as Lw= Log10(A) + Li. The area was modeled as a cylinder with radius equal to sensor to source Range (R) and the Height (H) equal to the surface of water to bottom of ocean in the area of seaquakes (1200 m). Thus A= $2*\pi*R^2$ + $H*2\pi*R$. The second model used was Source Level (SL). This log-scale model determines SL by measuring Receiver Level (RL) and adding the calculated Transmission Loss (TL), expressed as SL= RL + TL. The Bellhop 2D ray-tracing model was used to calculate the TL from source to sensor (Porter, 2011).

In addition to source and sensor location, the Bellhop model inputs the ocean environment including water sound speed depth profile, bottom sediment for absorbance, and bottom topography for propagation path. The model outputs TL, eigen rays, arrivals, and time-series. To run Bellhop, the study used the Acoustic Research Laboratory (ARL) underwater acoustic propagation modeling (UWAPM) toolbox. More information on the modeling and sample outputs are in Appendix.

The seaquake source power estimates obtained appear reasonable. The sound path from source to sensor consisted of multiple reflections. The Bellhop provided sound travel time of shortened eigen ray and TL as the sum of eigen rays and power diagram dBFS (full scale). The path profile resolution used was 1 km horizontal and 25 m vertical. The shortest path was used to estimate sound speed that was found to average 1492 +/- 9.6 m/s. The SL modeling can be improved by 1) increasing the path resolution, 2) averaging different paths as epicenter may vary a few kilometers given array bearing widths, and/or 3) using the Bellhop 3D model to include horizontally reflected energy.

The two models used to determine source power are compared in Figure 7B. The area model assumes uniform spread of power. This model gives the most conservative results but may give low estimates if obstructions are preventing reception of some of the transmission. The ray-tracing model considers power disruptions. The model can show too high TL if not all the ray paths are found. This can occur if inaccuracies exist in sensor or source locations, or bottom topography. The power calculation difference of path model (SL) and area model (PL) decrease with eigen rays detected. The SL model had similar results to the PL model when paths had 10 or more eigen rays (difference averaged 0.22 Lw dB re W/m^2). This confirms expectations that models have similar results when source power is not disrupted on its path to the receiver.

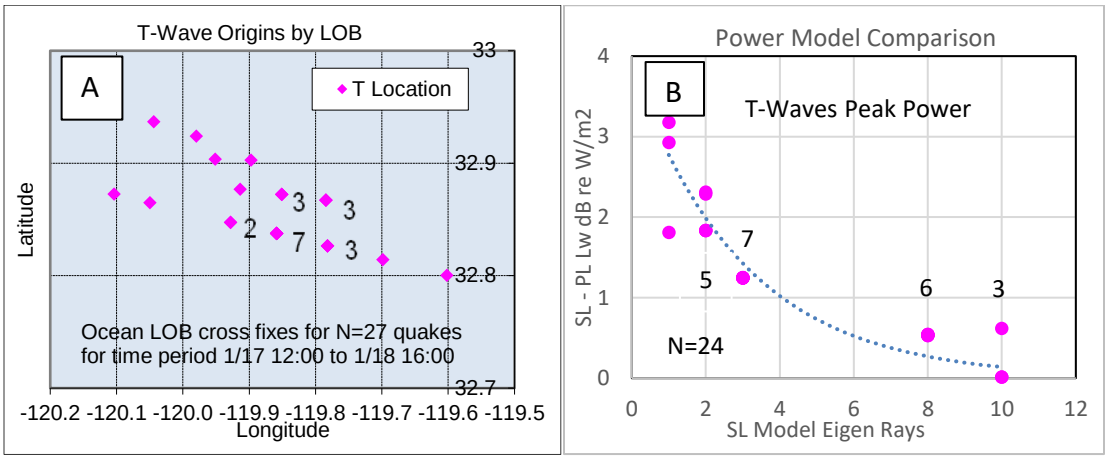

Figure 7. T-wave A) ocean origins and B) power models.

The seaquake magnitudes are of interest as this is the standard means of conveying event size. Because seismic sensors did not record the events, measuring magnitude requires another means. One means is to use an equation to convert source power to magnitude. We explored use of the P-wave equation found in our study. This gives an average magnitude of 4.23, with range 2.99 to 6.17 M_L. A problem is that while P-waves and seismic waves are measured from hypocenter the T-waves are measured from epicenter on seabed. We decided to use the equation $M_L = .031\ Lw - 3.30$ for ocean quakes (Dziak, 1997). This relation was confirmed by seismic data. It gives an average magnitude of 3.29 with range of 2.61 to 4.35 M_L. These values are reasonable.

There was interest in determining the magnitude and energy of all quakes detected. This can be approximated. All 71 P-waves were localized. Of 210 total T-waves, 27 were localized by cross fixing, 97 had one LOBs consistent with those localized, 3 events had different LOBs, and 83 had no LOB. We approximated acoustic SL of seaquakes without origin determination by using average values for range and TL. As shown in Figure 8, the 27 T-wave origins found by cross-fixing were in 14 cells and the centroids were used for positions. The figure is in tabular form to clarify calculations, but the beams were at angles. There were 7 North array bearings (number designations) and 5 South array bearings (letter designations) that had cross fixes. The average distance between fixes along bearing E is 7.93 km. Each cell (e.g. E-4) represents a sound path.

		North array								Avg	Avg	One
	LOBs	1	2	3	4	5	6	7	Total	R.km	TL.dB	LOB
South array	A			1					1	34.9	130.2	0
	B				1				1	34.8	138.1	3
	C				1	1			2	39.6	127.3	19
	D				1	3	3		7	50.8	124.5	18
	E	1	1	2	7	3	1	1	16	49.4	115.6	57
	Other											3
	Total	1	1	3	10	7	4	1	27	48.0	120.1	100

Note: 83 detections w/o LOB

Figure 8. T-waves LOB averages.

3.3 EARTHQUAKE MAPS

Earthquakes acoustically detected in this study were found in two areas. Of the quakes detected as T-waves, all 210 were at-sea (estimated M_L 2.2 to 6.5) and those detected as P-waves, (all 71) were on land (M_L 3.1 to 6.7). Different processes were used for event localization: P-waves were correlated with land-based seismic recordings; T-waves were localized by LOB intersection using two acoustic arrays, designated North and South. Due to the higher ground speed, P-waves are difficult to localize by LOBs. As shown in Figure 9, all P-wave origins were on land within 15 km of the earthquake epicenter. Figure 9 shows the 27 quakes localized by cross-fixing the two arrays. Seaquakes were 240 km southwest of the land earthquakes. T-waves had 127 LOBs detected at the South array and 27 at the North array. 97 quakes had LOBs from the South array that were not cross-fixed but consistent with those that were and another 3 were different. The quakes localized were of larger size. This suggests 59% (124 consistent bearings of 210 total detections) to 98% (124 consistent with 127 South array detections) of the seaquakes arose in the same general area.

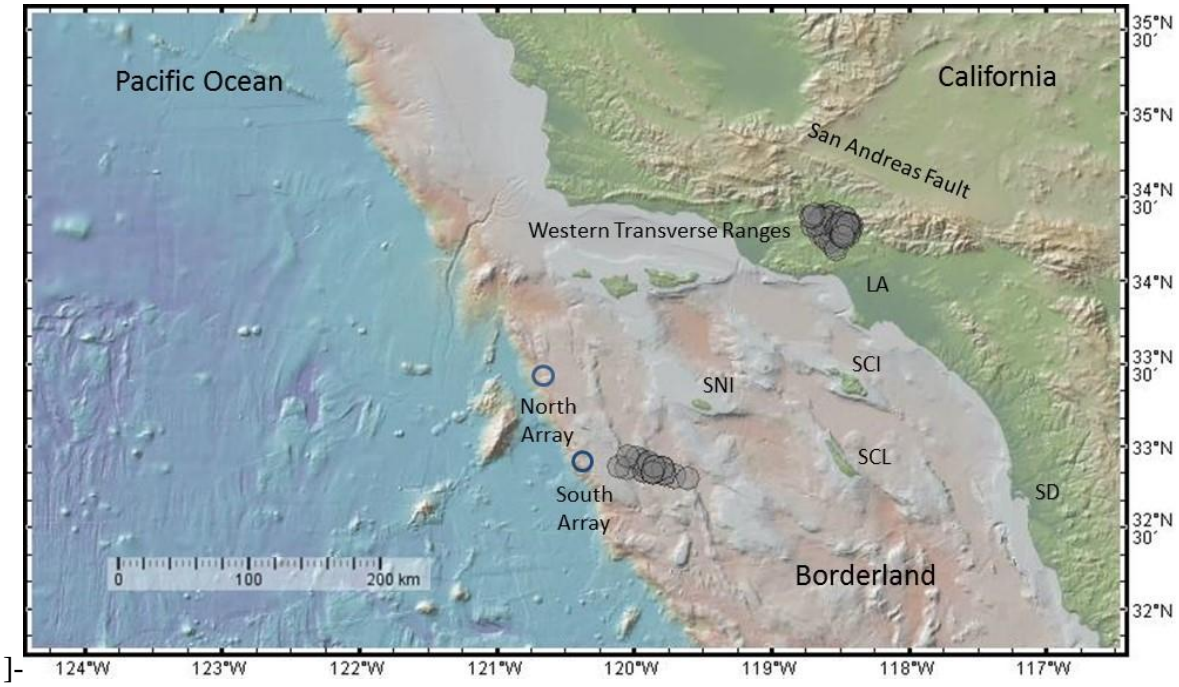

Figure 9. Quakes associated with 1994 Northridge earthquake.

A geographic map of quakes that were acoustically detected in this study shows both continental and ocean origin. The Global Multi-Resolution Topography (GMRT) map is used for illustration (Ryan, 2009). The graphics were made with GeoMapApp tools of Columbia University. The map acronyms are as follows: SNI = San Nicolas, SCI = Santa Catalina Island, SCL = San Clemente Island, LA = Los Angeles, and SD = San Diego. Two acoustic arrays were used in this study. Continental earthquakes are well documented with land seismic networks but ocean seaquakes are less documented. The data supporting Figure 9 is in Appendix Tables A1 and A2.

Prior studies show seaquakes in the inner Southern California Borderland that are in the SCSN catalog (Astiz, 2000; see Figure 4). The outer Borderland is at the western edge and beyond most current seismic coverage of the SCSN (Hutton, 2010; see Figure 10). Our study shows seaquakes

located along the Ferrelo Fault Zone in a major lateral offset not previously reported. This area is one of the largest active fault structures in the region, with bottom structures well preserved (Shepard and Emery, 1941). Sea floor morphology and seismic reflection studies below the ocean floor provide evidence of past tectonic activity in this region (Legg, 2015).

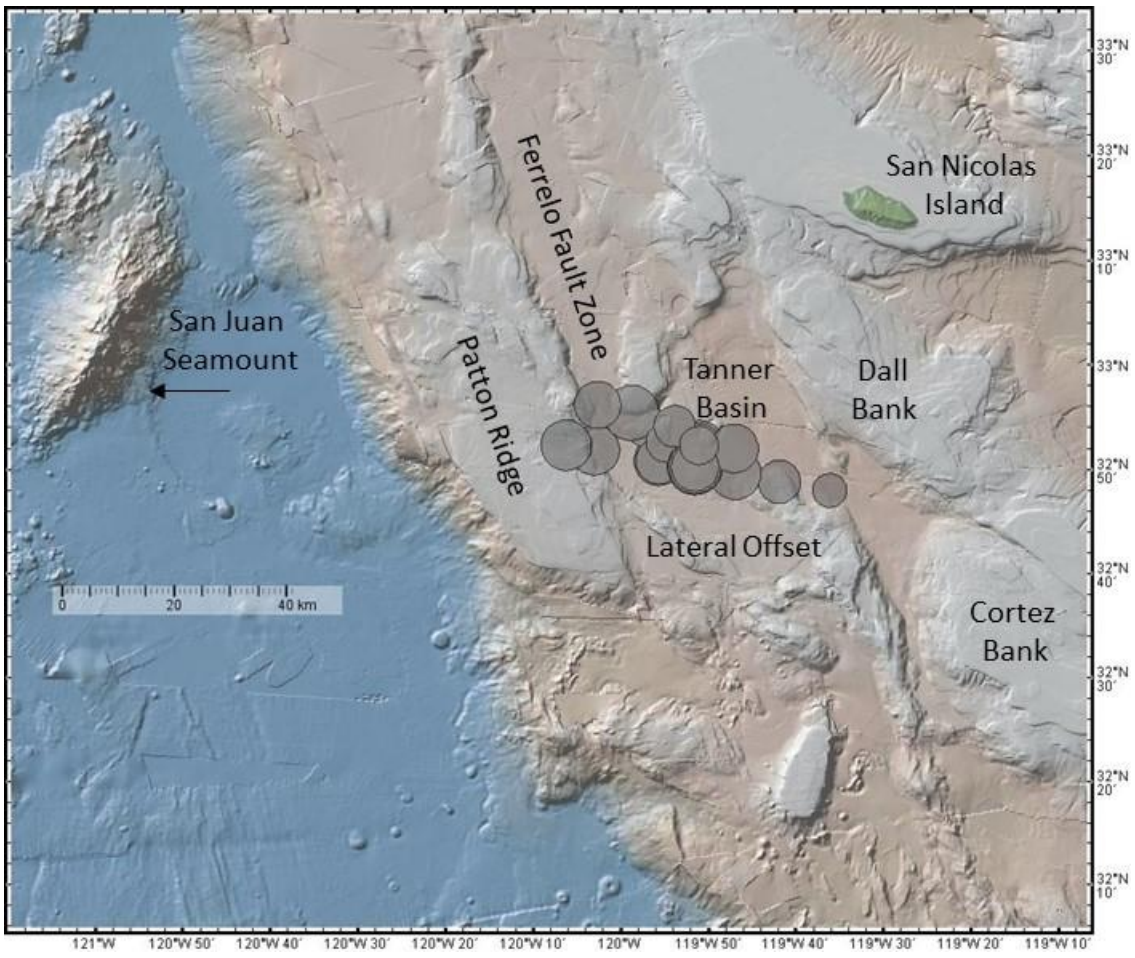

Figure 10. Seaquakes prior to 1994 Northridge earthquake.

Shown in Figure 10, are 27 quakes at sea detected as T-waves. There are a few reports of quakes in the outer Borderland such as a M_W 6.3 and aftershocks 40 km west of Patton Escarpment in 2012 but most quakes reported are in the inner Borderland. A review of offshore seismicity in the region is given (Hauksson, 2013; see Figure 2). The data supporting Figure 10 is in Appendix Table A-2.

3.4 DATA ANALYSIS

The study showed P-waves traveled through rock from hypocenters under Northridge, CA, and T-waves traveled through water from epicenters in Tanner Basin of the Outer Borderland. The datasets of all detected quakes were characterized with average values based on the localized subset as shown above in Figure 8. This enables approximation of the event sequence magnitudes and energy sums. The distribution of the acoustic events is shown in Figure 11A. T-waves had an average 3.5 M_L with standard deviation 0.41 and P-waves an average 3.9 M_L with standard deviation 0.54. Shown in

Figure 11B is a regression analysis of number of quakes, Log N, to magnitude (a log scale). The acoustic detections were consistent with findings for earthquakes showing a log-linear relationship of decreasing number of events with increasing size.

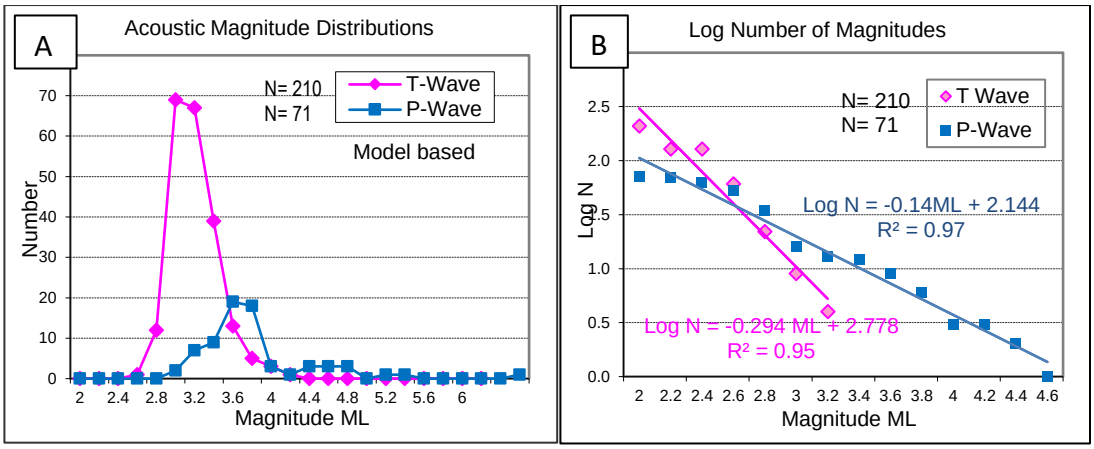

Figure 11. Acoustic event A) distributions and B) Log N regression

As in past studies, a relationship was found between the number N of events and the magnitude M that could be modeled in log-log space as a linear relation of the form Log N= a – bM. This equation has been derived for specific regions to predict the likelihood of earthquakes (Gutenberg, 1954) and used to estimate sensor thresholds (Fox, 1994). The relationship was computed with acoustic estimates of magnitude M_L. The log linear regressions by wave type are as follows:

T-waves: $\text{Log } N = -0.294\ M_L + 2.778$ $R^2 = .95$ (7)

P-waves: $\text{Log } N = -0.14\ M_L + 2.144$ $R^2 = .97$ (8)

Similarly, (graphic not shown) duration (D) in seconds decreased in a log N linear relationship. Of interest, T-wave duration was not found to correlate with magnitude M_L in this study and another (Astiz, 2000). However, T-wave duration was reported to correlate with magnitude M_W for certain regions and the variability may be due to consistency of acoustic energy conversion (Okal, 1986). The Log N equations for seaquake size relationship to durations were as follows:

T-waves: $\text{Log } N = -0.0066\ D + 2.533$ $R^2 = .92$ (9)

P-waves: $\text{Log } N = -0.0044\ D + 1.6568$ $R^2 = .90$ (10)

3.4.1 Earthquake Sequence

In this 80-hour study, data was partitioned into three periods. These were as follows: 1) initial period that likely represents normal activity, 2) quiet period of little activity, and 3) active period of main shock and aftershocks. As shown in Figure 12, T-wave activity changes prior to the 1994

Northridge earthquake and resumes afterwards. This is consistent with the stress recovery model discussed in association with the 1986 Oceanside earthquake (Hauksson, 1988; see Figure 13,).

Acoustic detection over time is shown as a scatter plot in Figure 12A. The number of detections per 2-hour intervals and associated energy (discussed later) is shown as a histogram in Figure 12B. The sequence of ocean and land quakes suggests a relationship. The conservation of energy requires, in a closed system, the potential energy and kinetic energy remain constant. We are not observing the whole system but nevertheless are observing transfer of energy through the region.

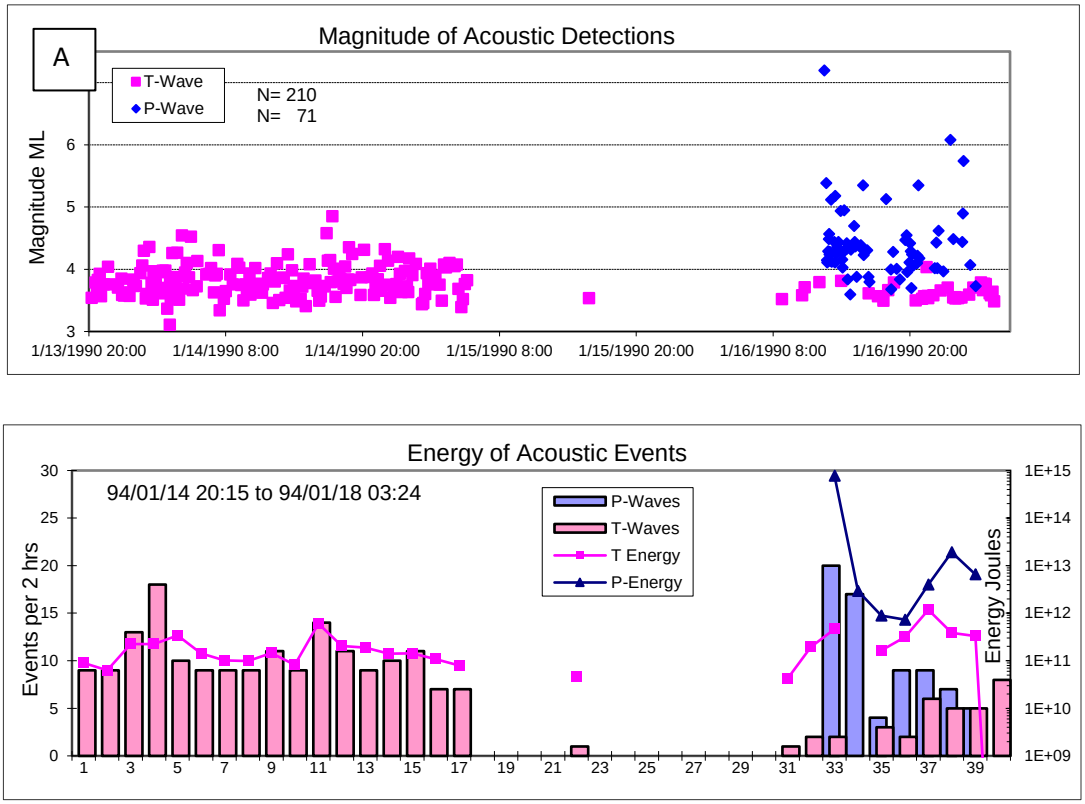

Figure 12. Sequence of Acoustic Detections.

The rebound theory states that earthquakes result from the sudden release of energy stored as elastic strain in tectonic plates. The energy propagates outward from the source as seismic and acoustic waves. The rebound theory process model consists of plate and fault dynamics (Ziv, 2007). Ocean hydrophones measure sound pressure fluctuations coupled to shock waves emanating from rock movements. The decline of observed T-wave activity might reflect accumulation of elastic strain in rocks off shore. If this interpretation is correct, then a rebalancing might be evident over a period of time. The sequence of seaquakes may be explained as a change of steady state.

3.4.2 Earthquake Energy

In this study, the acoustic waves were separated by type. It was found that all P-waves came from land with the hypocenter under Northridge, CA. It was found that all 210 T-waves detected came from the ocean with epicenter in outer borderland and 27 were localized. All 71 P-waves detected were localized with the hypocenters 0 to 18 Km deep. As shown in Table 5, the P-waves travel 200

km further but due to the higher velocity had similar travel times. Magnitudes were calculated using seismic sensor data. The P-waves had a higher average magnitude of 3.9 vs. 3.5 M_L. The P-waves ranged from 3.1 to 6.7 M_L while the T-waves ranged from 2.6 to 4.4 M_L.

Table 5. Acoustic detected and localized earthquakes.

Acoustic	Localized Earthquake Averages							
Measure	Number	Range	T. Time	Velocity	Intensity	Power	Duration	Magnitude
	Detected	Km	Seconds	Km/s	dB W/m2	dBW/s	Seconds	ML
P-waves	71	231.5	32.0	7.25	91.0	206.7	91.0	3.9
T-waves	27	32.6	32.6	1.49	94.1	195.7	125.9	3.5

Overall energy was estimated based on averages of localized events as previously discussed. Acoustic energy (Joules) was found by multiplying average source power (W/m2 per second) by duration (seconds). The average power (Watts) was found by dividing the total energy (Joules) by time period. Seismic energy was determined from magnitude and power by dividing energy total by time period (in seconds). As shown in Table 6, seismic energy was six orders of magnitude greater than acoustic energy. Seismic energy includes not only acoustically detected waves but rock displacement (acceleration) and heat due to friction. There was a 3-orders of magnitude decline in acoustic and seismic energy release from oceanic quakes during the quiet period of 31.3 hours. There was then a detection of continental energy and resumption of oceanic energy. This is not total energy. The calculations of energy only reflect earthquake detections made on study hydrophones in the Borderland, not that of all earthquakes detected on seismic networks.

Table 6. Energy of acoustic detected earthquakes.

Acoustic	Before Main Shock (Est)		After Main Shock (Est)	
Start Date-Time	94/01/14	94/01/16	94/01/17	94/01/17
End Date-Time	94/01/16	94/01/17	94/01/18	94/01/18
Types of waves	T-Wave	T-Wave	T-Wave	P-Wave
Events per hour	5.30	0.16	2.01	4.77
Acoustic Energy J	2.01E+08	1.78E+05	5.11E+05	1.82E+08
Acoustic Power W	1.70E+03	1.58E+00	9.54E+00	3.39E+03
Seismic Energy J	2.98E+12	2.97E+10	1.85E+11	8.10E+14
Seismic Power W	3.25E+14	3.41E+12	4.47E+13	1.96E+17

The elastic strain and associated potential energy states vary over long periods of time and may have different starting and ending values. Earthquake occurrence in one region transfers stress to adjacent regions. It has been calculated that the 1971 M 6.7 San Fernando earthquake increased stress at the 1994 Northridge rupture zone and contributed to the early onset of that earthquake (Stein, 1994). The stress reduction after an earthquake has a rapid onset, but may extend over a long period of time. In fact, for the 1994 Northridge earthquake, stress reduction to pre-earthquake levels occurred over two years (Zhao, 1997) to four years (Gasperini, 2009) after the main shock.

This page is intentionally blank.

4. DISCUSSION

4.1 MAJOR FINDINGS

This study showed changes in seaquake activity in the Southern California Borderland prior to the 1994 Northridge earthquake. Ocean sensors provided evidence of quakes not detected by land seismic sensors. Offshore quakes, detected as T-waves, occurred at a rate of 5.3 per hour for 33 hours and then abruptly stopped 31.3 hours prior to the main earthquake and then gradually resumed. Land quakes, detected as P-waves, were only observed after the earthquake (>M_L 3.0). The strength of P-waves was found by correlation with seismic events. The strength of T-waves weas estimated from peak amplitude, duration and by equation for converting power to magnitude. The ocean quakes were localized along the Ferrelo Fault Zone that is a known tectonically active area in the region. This study indicates current activity. There is horizontal movement of crustal blocks as well as vertical movement and compression. The San Juan Seamount nearby has had past volcanic activity and is associated with spreading and fractures (Bowden, 2016). The seaquakes originated along a 30-km major lateral offset. Decline of activity, stress buildup, and release is consistent with tectonic plate theory. A “logjam” model has been proposed for offshore deformation by obstruction of northwest directed block motion by a right-lateral strike-slip of western Transverse Ranges (Legg, 2015). Our findings are consistent with this model. Ocean quake activity was followed by land activity. Synchronization can occur between nearby faults, but rupture patterns of repeated earthquake clusters, while not exact repetitions, can show "fuzzy" synchrony (Scholz, 2010).

4.2 DATA QUALITY

An effort was made to ensure the acoustic detections were not man-made. The Bureau of Ocean Energy Management (BOEM) lists 23 oil and gas production facilitates in this region of federal waters. Recorders did not show facilities in area of study (checked 3 Aug 2017). The ocean platforms are off the coasts of Santa Barbara and Ventura counties north of 34^o Latitude. Google maps show locations. According to the California State Lands Commission (CSLC), there are four offshore oil platforms in state waters off the coast of California. They are platforms Holly in Santa Barbara County, Eva and Emmy in Huntington Beach, and Esther off Seal Beach. There are also four large man-made islands in Long Beach, and one off of Rincon Beach in Ventura County. Land seismic data was obtained online from SCEDC 1994.cat (http://www.scecdc.scec.org/ftp/catalogs/SCEC_DC/ 10 May 2017). The data is also available as waveform and parametric files from the Southern California Seismic Network (SCSN).

This page is intentionally blank.

5. CONCLUSIONS

This study shows the potential value of combining acoustic and seismic sensors for understanding the borderland regions to gain a more comprehensive understanding of the coastal geology. Tectonic activity predominates along coastal areas. This activity in the Pacific Ocean region is referred to as the Ring of Fire. Beyond the coastlines, there are many shallow water borderlands similar to that of the Southern California Borderland studied in this report. Seismic sensor networks are located predominately on land. Currently, these networks only detect limited inner borderland ocean seismic activity. Outer borderland regions are less studied but seismically active and should be investigated (Maloney, 2019). Hydrophones are sensitive to seismic activity and very useful for seaquake detection. Underwater seismic sensor can also be useful where deployed. Through data fusion of seismic and acoustic sensors, greater insight can be gained of regional earthquakes.

5.1 RECOMMENDATIONS

Our findings indicate current tectonic activity in the outer region of the Southern California Borderland, in a region not previously reported. Additional study is needed to better understand seismic activity in this region. It would be of interest to see if similar sound changes accompany other coastal earthquakes. It would also be of value to study other borderland regions and earthquake types (i.e., strike-slip and thrust faults). It is recommended that additional acoustic data be analyzed in the California Continental Borderland. If the observed phenomena are repeatable, the potential exists to set up a monitoring system to detect acoustic changes and perhaps enable early warning of earthquakes in the region. Analysis of other Borderland regions could prove valuable for understanding coastal earthquakes.

5.2 USEFUL RESOURCES

Marine Geoscience Data System (http://www.geomapapp.org) of Columbia University provides useful data and visualization tools. This was used for obtaining ocean environmental data input into the Bellhop ray trace model. U.S. Geological Survey has technical reports used for this study and keeps up to date records of earthquakes online (http://earthquake.usgs.gov). Wikipedia has acoustic documentation and useful equations for conversion of acoustic pressure, intensity and power (https://en.wikipedia.org/wiki/Sound_pressure). Wikipedia was used for common nomenclature symbols and some equations used in this report.

This page is intentionally blank.

REFERENCES

Aki, K. 1967, "Scaling Law of Seismic Spectrum," *Journal of Geophysical Research 72*(4): 1217–1231.

Astiz, L. and P. M. Shear, 2000, "Earthquake Locations in the Inner Continental Borderland, Offshore Southern California," *Bulletin of the Seismological Society of America*, 90(2).

Armstrong, B. H. 1969. "Acoustic Emission Prior to Rockbursts and Earthquakes," *Bulletin of the Seismological Society of America 59*(3):1259–1279.

Blackman, D., C. Nishimura, and J. Orcutt. 2000. "Seismoacoustic Recordings of a Spreading Episode on the Mohns Ridge," *Journal of Geophysical Research 105*. B5 (10), 10,961–10,973.

Baruah, Santanu, Saurabh Baruah, A. Kalita , R. Biswas , N. Gogoi , J. L. Gautam , M. Sanoujam and J. R. Kayal, 2012, "Moment magnitude – local magnitude relationship for the earthquakes of the Shillong-Mikir plateau, Northeastern India Region: a new perspective," *Geomatics, Natural Hazards and Risk*, 3:4, 365-375, DOI: 10.1080/19475705.2011.596577.

Bora, D. K., 2016, "Scaling relations of moment magnitude, local magnitude, and duration magnitude for earthquakes originated in northeast India," *Earthquake Science* 29(3):153–164, DOI 10.1007/s11589-016-0154-3.

Bowden, D. C., M. D. Kohler, V. C. Tsai, and D. S. Weerarante. 2016. "Offshore Southern California Lithospheric Velocity Structure from Noise-correlation Functions," *Journal of Geophysical Research: Solid Earth 121*:3415–3427. DOI: 10.1002/2016JB012919.

Butler, S. C. 2018, "Properties of Transducers: Underwater Sound Sources and Receivers," NUWC-NPT Technical Document 12,289.

Chouet, B. A. 1996. "Long-period Volcano Seismicity: Its Source and Use Eruption Forecasting," *Nature 380*(6572):309–316.

Choy, G. L., and J. L. Boatwright, 1995. "Global patterns of radiated seismic energy and apparent stress," *J. Geophys. Res*. 100(B9): 18,205-18,228.

Dziak, R., C. Fox, H. Matsumoto, and A. Schreiner. 1997. "The April 1992 Cape Mendocino Earthquake Sequence: Seismo-Acoustic Analysis Utilizing Fixed Hydrophone Arrays," *Marine Geophysical Research 19*(2):137–162.

Fischer, T. P., M. Morrissey, M. Calvache, D. Gomez, R. Torres, J. Stix, and S. Williams. 1994. "Correlations between SO2 Flux and Long-period Seismicity at Galeras Volcano," *Nature 368*(6467): 135–137.

Fox, C., R. Dziak, H. Matsumloto, and A. Schreiner 1994. "Potential for *Monitoring Low-level Hydrophone Arrays*," *Marine Technology Society Journal 27*(4): 22–30.

Freund, Friedemann. 2010 "Towards a Unified Solid State Theory for Pre-earthquake Signals," *Acta Geophysica 58*(5): 719-766. DOI: 10.2478/s11600-009-0066-x.

Gasperini, P. and B. Lolli, 2009. "An empirical comparison among aftershock decay models," *Physics of the Earth and Planetary* Interiors, 175: 183–193

Groot-Hedlin, C., and J. Orcutt, 1999. "Synthesis of e\Earthquake-generated T-Waves," *Geophysical Research Letters 26* (9): 1227–1230.

Gutenberg, B., and C. F. Richter, 1956. "Magnitude and Energy of Earthquakes," Annales Geophysicae *(Rome) 9*: 1–15.

Gutenberg, B., and C. F. Richter 1954. *Seismicity of the Earth and Associated Phenomena*. 2nd edition. Princeton University Press, Princeton, NJ.

Hammond, S., and D. Walker, 1991. "Ridge Event Detection: T-Phase Signals from the Juan de Fuca Spreading Center," *Marine Geophysical Research 13*(4): 331–348.

Hauksson, E., and L. M. Jones, 1988. "The July 1986 (M_L = 5.6) Oceanside Earthquake Sequence in the Continental Borderland, Southern California," *Bulletin of the Seismological Society of America*, 78(6): 1885-1906.

Hauksson, E., 2000. "Crustal Structure and Seismicity Distribution Adjacent to the Pacific and North America Plate Boundary in Southern California," *Journal of Geophysical Research* 105(B6): 13,875–13,903.

Hauksson, E., H. Kanamori, J. Stock, M.-H. Cormier, and M. Legg, 2013 "Active Pacific North America Plate boundary tectonics as evidenced by seismicity in the oceanic lithosphere offshore Baja California, Mexico," *Geophysical Journal International Advance Access,* DOI: 10.1093/gji/ggt467.

Hutton, K., J. Woessner, and E. Hauksson, 2010, "Earthquake Monitoring in Southern California for Seventy-Seven Years (1932–2008)," *Bulletin of the Seismological Society of America*, 100(2), DOI: 10.1785/0120090130

Ito, Aki, H. Sugioka, D. Suetsugu, H. Shiobara, T. Kanazawa, and Y. Fukao, 2012. "Detection of Small Earthquakes along the Pacific-Antarctic Ridge from T-wave Recorded by Abyssal Ocean-bottom Observatories," *Marine Geophysical Research* 33:229–238. DOI 10.1007/s11001-012-9158-0.

Johnson, R. H., and J. Northrop, 1966. "A Comparison of Earthquake Magnitude with T-Phase Strength," *Bulletin of the Seismological Society of America* 56(1):119–124.

Kedar, S., and H. Kanamori, 1996. "Continuous Monitoring of Seismic Energy Release Associated with the 1994 Northridge Earthquake and the 1992 Landers Earthquake," *Bulletin of the Seismological Society of America* 86(1A):255–258.

Lee, W. H., and Stewart SW (1981), Principles and Applications of Micro Earthquake Network: Advances in Geophysics, Supplement 2, Academic Press, Cambridge.

Legg, M. R., M. D. Kohler, N. Shintaku, and D. S. Weeraratne, 2015, "High-resolution Mapping of Two Large-scale Transpressional Fault Zones in the California Continental Borderland: Santa Cruz-Catalina Ridge and Ferrelo Faults," *Journal of Geophysical Research: Earth Surface 120*, 915–942. DOI: 10.1002/2014JF003322.

Lin, G., P. M. Shearer, and E. Hauksson, 2007. "Applying a Three-dimensional Velocity Model, Waveform Cross Correlation, and Cluster Analysis to Locate Southern California Seismicity from 1981 to 2005," *Journal of Geophysical Research: Solid Earth 112*, B12309. DOI: 10.1029/2007/JB004986.

Maloney, J. M., M. Legg, C. Nicholson, and T. K. Rockwell, 2019. "The California Continental Borderland SCEC White Paper.

McDonald, M. A., Hildebrand, J. A., Wiggins, S. E. and Ross, D., 2008. "A 50 Year comparison of ambient ocean noise near San Clemente Island: A bathymetrically complex coastal region off Southern California" *JASA* 124(4).

Nishimura, C., and D. Forsyth. 1989. "The Anisotropic Structure of the Upper Mantle in the Pacific," *Geophysical Journal International 96* Mark A.:203–229.

Okal, E., and J. Talandier. 1986. "T-wave Duration, Magnitudes and Seismic Moment of an Earthquake — Application to Tsunami Warning," *Journal of Physics of the Earth 34*(1):19–42.

Okal, E.A. 2007. "The Generation of T-waves by Earthquakes," *Advances in Geophysics 49*(1): 1–65.

Porter M.B., 2011, *The BELLHOP Manual and User's Guide: Preliminary Draft*. Heat, Light, and Sound Research, Inc.; San Diego, CA, USA.

Ryan, W.B.F., S. M. Carbotte, J. O. Coplan, S. O'Hara, A. Melkonian, R. Arko, R. A. Weissel, V. Ferrini, A. Goodwillie, F. Nitsche, J. Bonczkowski, and R. Zemsky. 2009. "Global Multi-resolution Topography Synthesis," *Journal of Geochemistry, Geophysics and Geosystems 10*(3): 1–9. Q03014 DOI: 10.1029/2008GC002332.

Scholz, C. 2010. "Large Earthquake Triggering, Clustering, and the Synchronization of Faults," *Bulletin of the Seismological Society of America* 100(3):901-909. DOI: 10.1785/0120090309.

Shepard, F. P., and K. O. Emery, 1941, "Submarine Topography off the Southern California Coast: Canyons and Tectonic Interpretation," *Geological Society of America Special Paper 31*.

Slack, P. 1999. "P-wave Detection Thresholds, Pn Velocity Estimates, and T-wave Location Uncertainty from Oceanic Hydrophones," *Journal of Geophysical Research* 104 (B6)S: 13,061–13,072.

Stephen, R. A., S. T. Bolmer, I. A. Udovydchenkov, P. F. Worcester, M. A. Dzieciuch, R. K. Andrew, J. A. Mercer, J. A. Colosi, and B. M. Howe. 2013. "Deep Seafloor Arrivals in Long Range Ocean Acoustic Propagation," *Journal of the Acoustical Society of America 134* (4), Part 2:3307–3317.

Stein, R., G. C. P. King, and J. Lin, 1994. "Stress Triggering of the 1994 M=6.7 Northridge, California, Earthquake by Its Predecessors," *Science 265*:1333–1496.

Ten Brink, U. S., Zhang, Jie, Brocher, T.M., Okaya, D. A., Klitgord, K. D., Fuis, G. S., 2000, "Geophysical evidenc for the evolution of the California Inner Continental Borderland as a metamorphic core complex," *Journal of Geophysical Research* 105(B3) pp 5835-5875.

Urich, R. J., "Ambient Noise in the Sea", NAVSEA Report AD460546 1984, DTIC https://apps.dtic.mil/sti/pdfs/ADA460546.pdf

Williams, C. M., R. A. Stephen, and D. K. Smith, 2006. "Hydroacoustic Events Located at the Intersection of the Atlantis (30°N) and Kane (23°40'N) Transform Faults with the Mid-Atlantic Ridge," *Journal of Geochemistry, Geophysics and Geosystems 7(6)*. DOI: 10.1029/2005GC001127.

Zhao, D., H. Kanamori, and D. Wiens. 1997. "State of Stress Before and After the 1994 Northridge Earthquake," *Geophysical Research Letters 24*(r):519–522.

Ziv, A., A. Cochard and J. Schmittbuhl, 2007, "Does Elastic Rebound Theory Apply to Seismic Faults?" p. 51 in *Earthquakes and Acoustic Emission* Carpinteri & Lacidogna (eds) Taylor and Francis Group, London, ISBN 978-0-415-44402-6.

This page is intentionally blank.

APPENDIX

ADDITIONAL CHARTS AND TABLES

A.1 OVERVIEW

Items included in this section are:

A.2 OVERVIEW OF STUDY METHODS

The study used acoustic and seismic data. Figure A-1 shows a diagram of steps taken in the study: 1. record land earthquake acoustic detections and compare with seismic data, 2. find land earthquake power and magnitude (P-waves), 3. find ocean seaquake locations and sound paths (T-waves), and 4. model ocean acoustic source power and equivalent seismic magnitude. For the 80-hour study period, calculate acoustic and seismic power dissipation (Watts) and energy (Joules).

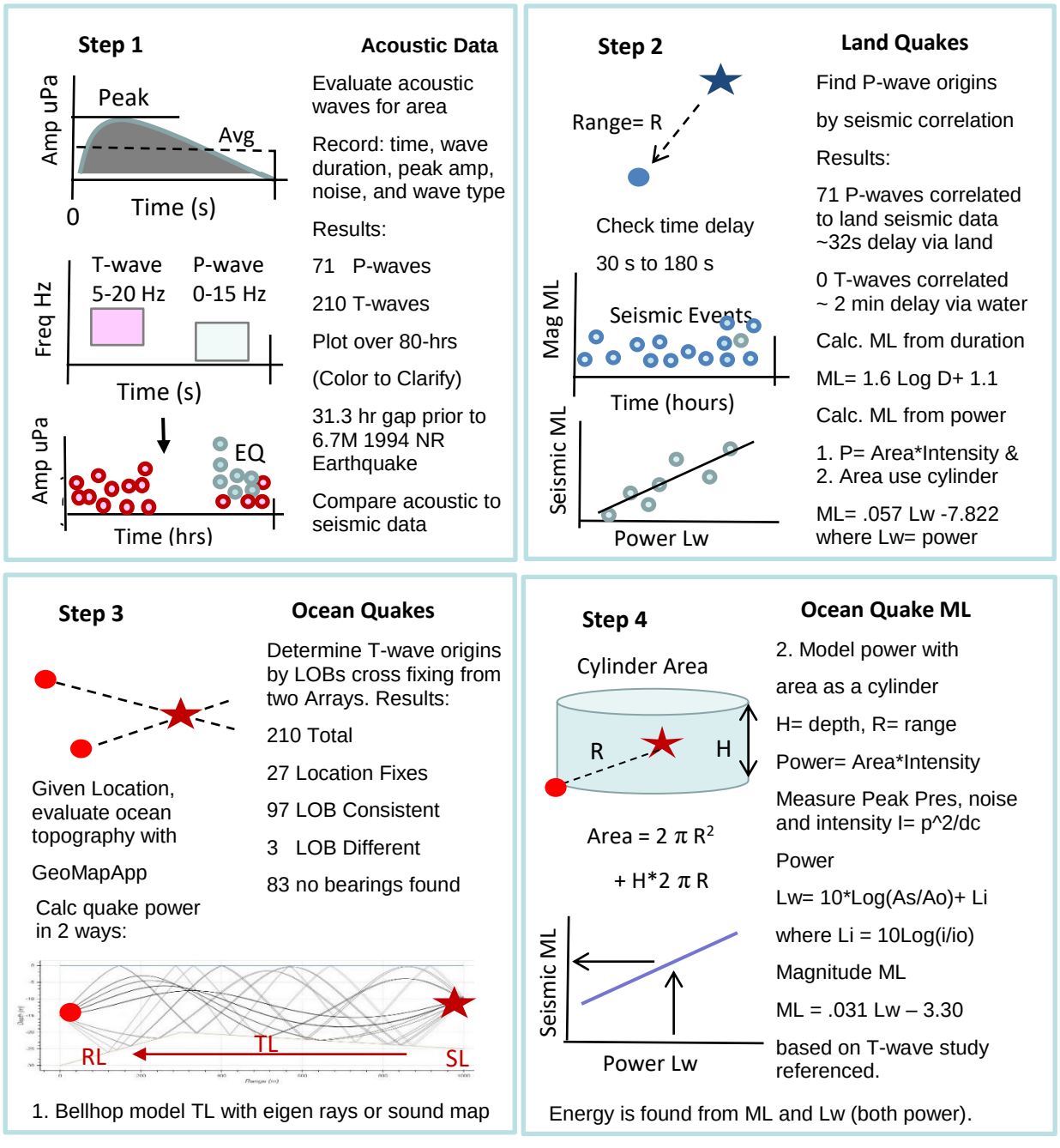

Figure A-1. Diagram of steps taken in study.

A.3 SOURCE POWER CALCULATIONS

Source power calculations were made in two ways for P-waves and T-waves. For P-waves, the methods used were 1) area model, Power= Area*Intensity and 2) acoustic duration correlation with seismic magnitude (a form of power). P-waves traveled through land. The area model used was a cylinder with radius equal to range from sensor to quake and height equal to crustal depth (24 Km). The source power calculations were close to the magnitudes determined by seismic networks. For T-waves, the methods used were 1) area model, and 2) ray-trace model using Bellhop. T-waves traveled through water. The area model used was a cylinder with radius equal to range from sensor to quake and height equal to average depth (1200 m). The results of these methods were similar when 10 or more eigen rays were found. Ray trace modeling factors in the ocean bottom profile.

A.4 BELLHOP MODEL CALCULATIONS

Shown in Figure A-2 is one output. The diagrams show A) rays from source (left) to sensor (right) and B) corresponding sound power in dBFS (colored). This run showed 8 eigen ray paths from source to receiver. In this output there were 8 eigen rays. Ray tracing model used the Bellhop 2D model obtained from ARL. Python was used as part of Anaconda software suite run on Windows computer. The acoustic toolbox (at file) was downloaded. ArlPy code includes Numpy, Pandas and MatPlotLib for graphic outputs and supporting analysis. The Under Water Acoustic Propagation Modeling Toolbox (UWAPM) was used to create parameters for the Bellhop model.

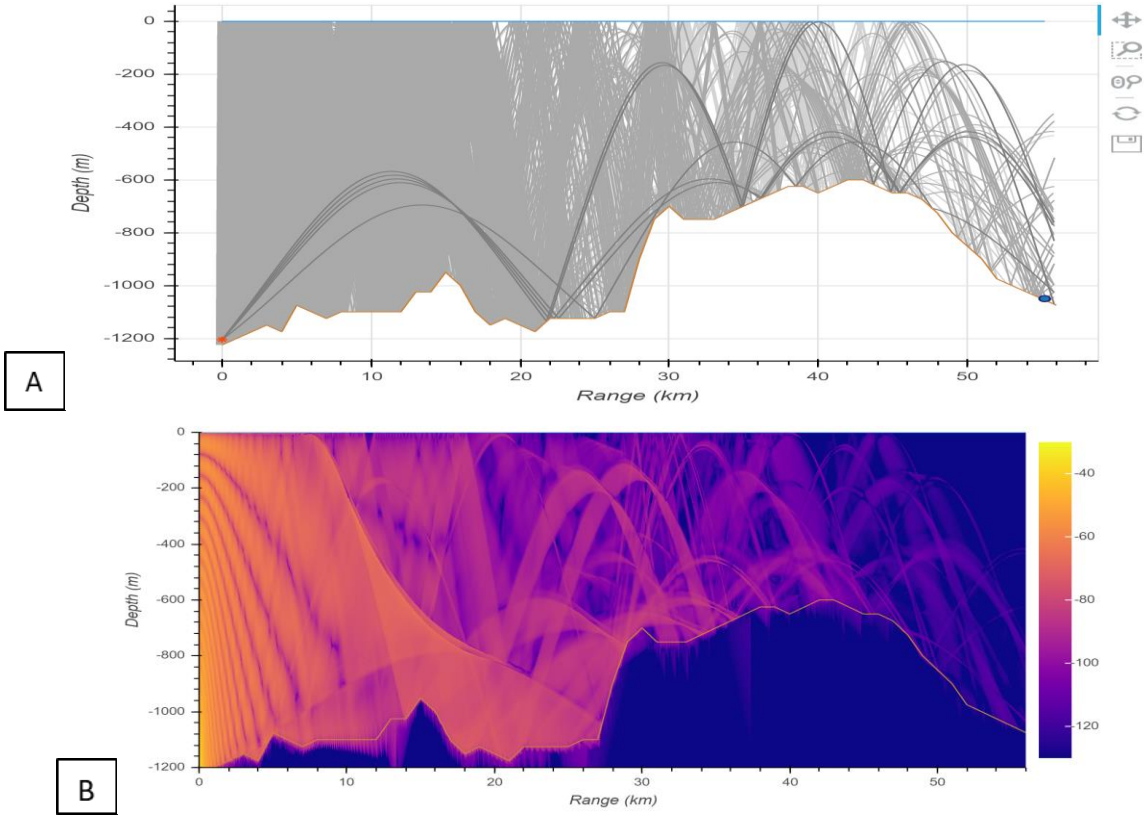

Figure A-2. Bellhop model: A) ray traces and B) energy.

A.5 ACOUSTIC P-WAVE CALCULATIONS

P-waves detected on acoustic hydrophones were found to correlate with land quakes recorded by seismic networks. There was a time delay consistent for travel through land (7.25 Km/s average using slant range XYZ). Table A-1 shows some of the values measured and calculated for 71 P-waves localized. Quake origins are from corresponding seismic data taken from SCEDC. The area model for energy dissipation was used to determine acoustic power at source (P= A*I). The knowledge of seismic magnitudes at origin enabled comparison by regression analysis. The equation for magnitude (M_L) given acoustic power (Lw) for P-waves is M_L = .0567 Lw – 7.8221. Earthquake power levels were used for calculation of acoustic and seismic energy levels.

Table A-1. Acoustic P-waves localized.

Acoustic Sensor													Quake Origin (Seismic)				
Date/Time Observed	Wave Type	Pres dBuPa	Dura-tion s	Noise dBuPa	Travel Time s	Range XY Km	Velocity Km/s	Peak Li dBw/m	Area As at R&H	Power P=A*I	ML est Power	MLest Dur(s)	Date/Time Origin	Lat	Lon	Depth Km	ML Seismic
1994/01/17 12:31:27	P	121.6	523	71.6	32	222.7	7.0	121.5	3.5E+11	165.4	5.71	5.46	94/01/17 12:30:55	34.21	-118.54	18.2	6.70
1994/01/17 12:40:12	P	109.8	340	71.6	32	226.3	7.1	109.6	3.6E+11	153.6	5.01	5.16	94/01/17 12:39:40	34.26	-118.54	5.9	4.89
1994/01/17 12:44:04	P	94.0	93	77.0	28	227.0	8.1	93.9	3.6E+11	132.4	3.77	4.26	94/01/17 12:43:36	34.35	-118.63	5.3	3.65
1994/01/17 12:46:32	P	85.1	54	76.9	30	236.2	7.9	85.0	3.9E+11	124.0	3.28	3.88	94/01/17 12:46:02	34.3	-118.44	5.5	3.61
1994/01/17 12:51:38	P	90.7	51	76.9	33	237.0	7.2	90.6	3.9E+11	129.6	3.61	3.84	94/01/17 12:51:05	34.33	-118.46	5.9	3.79
1994/01/17 12:55:07	P	92.6	62	76.5	33	235.5	7.1	92.5	3.8E+11	131.8	3.74	3.98	94/01/17 12:54:34	34.31	-118.46	5.9	3.99
1994/01/17 12:56:18	P	93.5	55	76.5	31	225.0	7.3	93.4	3.5E+11	132.3	3.77	3.89	94/01/17 12:55:47	34.28	-118.58	5.9	4.07
1994/01/17 12:58:29	P	74.9	43	75.6	32	240.5	7.5	89.1	4.0E+11	129.5	3.60	3.72	94/01/17 12:57:57	34.35	-118.43	5.8	3.74
1994/01/17 12:59:58	P	88.9	43	75.6	28	235.6	8.4	88.8	3.8E+11	129.0	3.58	3.72	94/01/17 12:59:30	34.33	-118.48	5.5	3.78
1994/01/17 13:01:35	P	88.9	51	75.1	34	227.6	6.7	88.8	3.6E+11	129.2	3.59	3.84	94/01/17 13:01:01	34.35	-118.62	5.5	3.64
1994/01/17 13:06:59	P	99.6	86	75.0	31	234.6	7.6	99.5	3.8E+11	140.3	4.24	4.21	94/01/17 13:06:28	34.38	-118.55	5.9	4.62
1994/01/17 13:09:09	P	88.1	51	75.0	34	224.9	6.6	87.9	3.5E+11	128.4	3.54	3.84	94/01/17 13:08:28	34.25	-118.55	5.9	3.62
1994/01/17 13:23:22	P	89.2	59	73.2	32	228.4	7.1	89.1	3.6E+11	131.5	3.72	3.94	94/01/17 13:22:50	34.36	-118.62	5.7	3.94
1994/01/17 13:25:44	P	85.3	39	73.2	33	233.5	7.1	85.2	3.8E+11	127.8	3.51	3.66	94/01/17 13:25:11	34.33	-118.51	5.7	3.61
1994/01/17 13:27:19	P	105.0	195	75.2	34	236.2	6.9	104.8	3.9E+11	145.5	4.54	4.77	94/01/17 13:26:45	34.32	-118.46	5.9	4.68
1994/01/17 13:32:53	P	91.8	66	75.2	32	236.9	7.4	91.7	3.9E+11	132.3	3.77	4.02	94/01/17 13:32:21	34.31	-118.44	5.7	3.75
1994/01/17 13:38:18	P	91.3	55	71.0	30	228.3	7.6	91.2	3.6E+11	135.8	3.98	3.89	94/01/17 13:37:48	34.35	-118.61	5.7	3.86
1994/01/17 13:45:08	P	86.1	28	73.3	34	232.3	6.8	86.0	3.7E+11	128.4	3.54	3.43	94/01/17 13:44:34	34.35	-118.55	5.5	3.84
1994/01/17 13:45:45	P	89.2	59	73.3	31	230.7	7.4	89.0	3.7E+11	131.4	3.72	3.94	94/01/17 13:45:14	34.39	-118.62	5.5	3.94
1994/01/17 13:56:33	P	106.8	125	72.0	31	223.1	7.2	106.7	3.5E+11	150.1	4.81	4.47	94/01/17 13:56:03	34.29	-118.62	5.9	4.44
1994/01/17 14:04:33	P	87.3	47	72.0	33	227.8	6.9	87.1	3.6E+11	127.3	3.48	3.79	94/01/17 14:04:00	34.36	-118.63	5.7	3.66
1994/01/17 14:07:29	P	90.1	51	75.4	33	230.7	7.0	90.0	3.7E+11	129.3	3.59	3.84	94/01/17 14:06:56	34.31	-118.53	6.4	3.53
1994/01/17 14:08:41	P	87.2	54	76.4	33	240.4	7.3	87.1	4.0E+11	129.7	3.62	3.88	94/01/17 14:08:08	34.33	-118.41	5.6	3.77
1994/01/17 14:15:05	P	95.3	82	73.4	34	238.3	7.0	95.1	3.9E+11	138.8	4.15	4.17	94/01/17 14:14:31	34.33	-118.44	5.9	4.45
1994/01/17 14:27:24	P	92.6	62	72.2	32	240.0	7.5	92.5	4.0E+11	135.5	3.96	3.98	94/01/17 14:26:52	34.38	-118.47	5.2	3.83
1994/01/17 14:28:34	P	94.4	62	73.0	30	222.0	7.4	94.3	3.4E+11	136.7	4.03	3.98	94/01/17 14:28:04	34.19	-118.53	16.7	3.92
1994/01/17 14:34:14	P	86.6	16	73.0	32	234.1	7.3	86.5	3.8E+11	129.0	3.58	3.04	94/01/17 14:33:42	34.31	-118.48	1.9	3.34
1994/01/17 14:46:27	P	84.6	31	73.3	32	221.0	6.9	84.5	3.4E+11	122.6	3.20	3.50	94/01/17 14:45:55	34.29	-118.65	5.9	3.10
1994/01/17 14:51:10	P	91.2	42	77.2	32	234.8	7.3	91.1	3.8E+11	134.0	3.87	3.71	94/01/17 14:50:38	34.31	-118.47	2.3	3.82
1994/01/17 15:07:34	P	98.6	105	72.9	31	234.1	7.6	98.5	3.8E+11	142.7	4.38	4.34	94/01/17 15:07:03	34.3	-118.47	2.4	4.20
1994/01/17 15:10:45	P	94.1	59	71.6	33	235.5	7.1	94.0	3.8E+11	135.7	3.97	3.94	94/01/17 15:10:12	34.31	-118.46	5.8	3.94
1994/01/17 15:14:59	P	90.8	31	74.1	32	238.4	7.5	90.7	3.9E+11	134.1	3.87	3.50	94/01/17 15:14:27	34.35	-118.46	5.8	3.87
1994/01/17 15:21:26	P	85.3	43	72.5	35	229.8	6.6	85.2	3.7E+11	130.6	3.67	3.72	94/01/17 15:20:51	34.37	-118.61	5.7	3.38
1994/01/17 15:42:45	P	90.9	62	70.2	33	238.3	7.2	90.8	3.9E+11	134.6	3.90	3.98	94/01/17 15:42:12	34.31	-118.42	1.9	3.89
1994/01/17 15:45:43	P	94.9	117	72.1	31	233.4	7.5	94.7	3.8E+11	135.4	3.95	4.42	94/01/17 15:45:12	34.37	-118.62	5.7	3.84
1994/01/17 15:54:43	P	107.7	133	75.1	32	229.3	7.2	107.6	3.6E+11	149.7	4.79	4.51	94/01/17 15:54:11	34.38	-118.63	12.5	4.85
1994/01/17 15:57:59	P	86.6	39	73.5	32	232.7	7.3	86.5	3.8E+11	128.7	3.56	3.66	94/01/17 15:57:27	34.3	-118.49	9.9	3.73
1994/01/17 16:16:34	P	90.7	51	73.5	32	232.7	7.3	90.6	3.8E+11	133.7	3.85	3.84	94/01/17 16:16:02	34.29	-118.48	2.8	3.81
1994/01/17 16:23:20	P	87.3	16	72.6	33	239.0	7.2	87.1	3.9E+11	131.3	3.71	3.04	94/01/17 16:22:47	34.33	-118.43	0.8	3.38

1994/01/17 16:27:40	P	86.3	39	71.8	33	227.8	6.9	86.2	3.6E+11	128.5	3.55	3.66	94/01/17 16:27:08	34.36	-118.63	5.7	3.30
1994/01/17 17:56:38	P	109.1	137	73.3	30	228.7	7.6	109.0	3.6E+11	150.0	4.80	4.53	94/01/17 17:56:08	34.23	-118.57	19.1	4.63
1994/01/17 18:20:54	P	82.7	20	73.3	30	232.6	7.8	82.6	3.7E+11	124.1	3.29	3.19	94/01/17 18:20:24	34.28	-118.47	11.3	3.50
1994/01/17 18:23:25	P	83.9	20	71.3	30	227.9	7.6	83.8	3.6E+11	126.9	3.45	3.19	94/01/17 18:22:55	34.37	-118.64	11.3	3.18
1994/01/17 18:32:39	P	92.4	47	73.0	30	230.5	7.7	92.3	3.7E+11	135.7	3.97	3.79	94/01/17 18:32:09	34.28	-118.5	2.8	3.78
1994/01/17 18:51:41	P	87.5	43	74.6	33	240.0	7.3	87.3	4.0E+11	132.5	3.78	3.72	94/01/17 18:51:08	34.34	-118.43	-0.4	3.51
1994/01/17 19:07:57	P	85.5	20	75.0	28	227.5	8.1	85.4	3.6E+11	128.5	3.55	3.19	94/01/17 19:07:29	34.34	-118.61	5.9	3.34
1994/01/17 19:36:08	P	90.4	70	74.2	34	235.5	6.9	90.2	3.8E+11	130.7	3.68	4.06	94/01/17 19:35:34	34.31	-118.46	2.1	3.97
1994/01/17 19:44:21	P	100.2	120	72.5	28	227.9	8.2	100.0	3.6E+11	144.4	4.48	4.44	94/01/17 19:43:53	34.37	-118.64	13.3	4.05
1994/01/17 19:46:53	P	85.7	39	72.2	31	228.7	7.4	85.6	3.6E+11	129.9	3.63	3.66	94/01/17 19:46:22	34.38	-118.64	5.5	3.46
1994/01/17 19:59:21	P	84.9	31	72.1	32	228.5	7.1	84.8	3.6E+11	127.2	3.47	3.50	94/01/17 19:58:49	34.37	-118.63	5.5	3.61
1994/01/17 20:02:36	P	90.7	47	70.9	30	236.2	7.9	90.5	3.9E+11	130.8	3.68	3.79	94/01/17 20:02:06	34.41	-118.56	5.4	3.92
1994/01/17 20:06:00	P	87.4	51	72.4	32	232.8	7.3	87.3	3.8E+11	132.8	3.80	3.84	94/01/17 20:05:28	34.33	-118.52	5.8	3.79
1994/01/17 20:08:39	P	85.5	20	75.3	30	231.9	7.8	85.4	3.7E+11	128.9	3.57	3.19	94/01/17 20:08:09	34.26	-118.46	22.7	3.20
1994/01/17 20:12:26	P	91.9	43	71.2	37	233.5	6.3	91.8	3.8E+11	132.7	3.79	3.72	94/01/17 20:11:49	34.32	-118.5	2	3.74
1994/01/17 20:18:26	P	84.5	20	71.2	36	236.2	6.6	84.4	3.9E+11	124.9	3.34	3.19	94/01/17 20:17:50	34.29	-118.43	1.9	3.56
1994/01/17 20:38:56	P	93.5	27	73.2	32	235.5	7.4	93.4	3.8E+11	135.7	3.97	3.40	94/01/17 20:38:24	34.31	-118.46	2.3	3.60
1994/01/17 20:40:10	P	90.1	23	75.6	31	232.7	7.5	90.0	3.8E+11	130.7	3.68	3.29	94/01/17 20:39:38	34.29	-118.48	2.7	3.72
1994/01/17 20:46:33	P	116.5	236	70.2	31	227.2	7.3	116.4	3.6E+11	159.7	5.37	4.91	94/01/17 20:46:03	34.3	-118.57	5.8	4.85
1994/01/17 20:50:58	P	88.1	43	72.2	35	236.4	6.8	88.0	3.9E+11	131.7	3.73	3.72	94/01/17 20:50:23	34.35	-118.49	5.8	3.68
1994/01/17 22:11:39	P	85.7	20	74.9	33	222.2	6.7	85.6	3.4E+11	127.5	3.49	3.19	94/01/17 22:11:06	34.26	-118.6	-0.3	3.52
1994/01/17 22:19:57	P	92.2	59	75.3	33	229.2	7.0	92.1	3.6E+11	135.4	3.95	3.94	94/01/17 22:19:24	34.37	-118.62	11.2	3.93
1994/01/17 22:25:08	P	84.7	40	73.5	35	232.2	6.6	84.6	3.7E+11	127.7	3.50	3.67	94/01/17 22:24:33	34.34	-118.54	0.4	3.52
1994/01/17 22:32:28	P	91.2	86	73.5	34	239.1	7.0	91.0	4.0E+11	133.8	3.86	4.21	94/01/17 22:31:54	34.34	-118.44	5.7	4.12
1994/01/17 22:57:47	P	90.2	55	75.0	33	228.3	6.9	90.1	3.6E+11	133.3	3.83	3.89	94/01/17 22:57:14	34.35	-118.61	8.8	3.47
1994/01/17 23:34:02	P	121.6	480	72.2	31	220.8	7.1	121.5	3.4E+11	164.9	5.68	5.40	94/01/17 23:33:31	34.33	-118.7	9.1	5.58
1994/01/17 23:49:57	P	93.1	94	72.2	32	223.6	7.0	92.9	3.5E+11	135.1	3.93	4.27	94/01/17 23:49:25	34.34	-118.67	7.7	3.99
1994/01/18 0:36:48	P	93.9	59	76.2	27	231.2	8.6	93.8	3.7E+11	138.4	4.13	3.94	94/01/18 00:36:21	34.27	-118.48	12.4	3.94
1994/01/18 0:40:07	P	95.8	82	74.4	32	233.9	7.3	95.7	3.8E+11	138.7	4.14	4.17	94/01/18 00:39:35	34.38	-118.56	6.5	4.40
1994/01/18 0:43:40	P	113.9	211	73.7	31	224.8	7.3	113.7	3.5E+11	154.8	5.08	4.83	94/01/18 00:43:09	34.38	-118.7	10.7	5.24
1994/01/18 1:18:25	P	89.4	43	72.5	34	224.2	6.6	89.3	3.5E+11	133.0	3.81	3.72	94/01/18 01:17:51	34.38	-118.71	11.5	3.57
1994/01/18 1:46:31	P	85.3	23	72.1	36	227.0	6.3	85.2	3.6E+11	129.6	3.61	3.29	94/01/18 01:45:55	34.4	-118.69	3.1	3.23
Min		74.9	16.0	70.2	27.0	220.8	6.3	78.5	3.4E+11	194.2	3.2	3.0		34.2	-118.7	-0.4	3.1
Max		121.6	523.0	77.2	37.0	240.5	8.6	121.5	4.0E+11	236.9	5.6	5.5		34.4	-118.4	22.7	6.7
Avg		91.0	77.9	73.6	32.0	231.4	7.3	91.0	3.7E+11	206.7	3.9	3.9		34.3	-118.5	6.5	3.9

A.6 ACOUSTIC T-WAVE CALCULATIONS

T-waves detected on acoustic hydrophones did not correlate with land quakes. Using two array LOB cross-fixing, 27 quakes were found to arise in the ocean in the Southern California Borderland. There was a time delay consistent for travel through water (1,494 m/s average determined by time delay of eigen rays using Bellhop model). Table A-2 shows some of the values measured and calculated for T-waves localized. There was no seismic sensor magnitude data to correlate with acoustic sensors. The seismic magnitude (M_L) were determined from acoustic source power (Lw) using equation $M_L = .031\ Lw - 3.30$ (Dziak, 1997). The localized seaquake data shown was used for estimating magnitudes, power and energy values for all 210 T-waves detected.

Table A-2. Acoustic T-waves localized.

Acoustic Sensor						Quake Origin											
Date/Time Quake Observed	Wave Type	RL Lp dBuPa	Dura (s)	Noise dBuPa	Intensity dBwm2	Lat Fix	Lon Fix	Dist Km	Depth m	Area in m^2	TL Li dBuPa	SL Li dBuPa	Date/Time Quake Origin	Power P=A*I	ML P=A*I	ML P=SL	Eigen Rays
1994/01/15 1:19:40	T	96.7	199	76.1	96.6	32.85	-119.93	42.17	1200	1.1E+10	135	231.0	94/01/15 01:19:12	124.0	3.3	3.9	0
1994/01/15 1:42:02	T	95.9	129	76.3	95.8	32.84	-119.86	48.70	1025	1.5E+10	123.2	145.4	94/01/15 01:41:29	124.1	3.3	3.5	3
1994/01/15 2:53:10	T	88.8	35	71.5	88.6	32.87	-119.78	55.21	1200	2.0E+10	112.2	126.2	94/01/15 02:52:42	116.9	2.9	2.9	8
1994/01/15 3:07:18	T	92.7	35	75.6	92.6	32.90	-119.95	34.78	1100	7.9E+9	99.2	117.1	94/01/15 03:06:54	116.8	2.9	2.6	10
1994/01/15 3:21:20	T	93.9	254	73.9	93.7	32.85	-119.93	42.17	1200	1.1E+10	135	227.9	94/01/15 03:20:52	120.7	3.1	3.8	0
1994/01/15 3:46:17	T	95.5	141	75.6	95.4	32.87	-119.85	48.92	1125	1.5E+10	133.3	155.5	94/01/15 03:45:43	124.1	3.3	3.8	2
1994/01/15 4:11:20	T	99.0	129	78.3	98.9	32.86	-120.05	35.20	1150	8.0E+9	138.6	162.1	94/01/15 04:10:56	122.6	3.2	4.0	2
1994/01/15 4:28:12	T	95.5	218	75.4	95.4	32.84	-119.86	48.70	1000	1.5E+10	123.2	142.9	94/01/15 04:27:39	121.6	3.1	3.4	3
1994/01/15 4:58:52	T	98.8	238	79.9	98.7	32.92	-119.98	34.78	925	7.9E+9	138.1	161.9	94/01/15 04:58:28	122.8	3.2	4.0	2
1994/01/15 5:31:49	T	90.0	140	71.3	89.9	32.88	-119.91	43.00	1025	1.2E+10	135	223.7	94/01/15 05:31:19	118.5	3.0	3.6	0
1994/01/15 9:03:29	T	90.5	94	72.4	90.4	32.87	-119.85	48.92	1125	1.5E+10	133.3	148.8	94/01/15 09:02:56	117.4	2.9	3.6	2
1994/01/15 9:33:51	T	97.0	133	76.1	96.9	32.87	-120.10	25.46	775	4.3E+9	106.9	132.4	94/01/15 09:33:34	121.9	3.2	3.0	10
1994/01/15 9:53:08	T	96.2	78	74.4	96.1	32.83	-119.78	56.02	1150	2.0E+10	112.1	135.8	94/01/15 09:52:30	126.8	3.4	3.1	8
1994/01/15 11:11:50	T	96.0	78	75.8	95.9	32.83	-119.78	56.02	1150	2.0E+10	112.1	133.9	94/01/15 11:11:12	124.9	3.3	3.1	8
1994/01/15 12:10:01	T	90.9	31	71.3	90.8	32.87	-119.78	55.21	1100	2.0E+10	112.2	130.6	94/01/15 12:09:23	121.3	3.1	3.0	8
1994/01/15 13:28:26	T	93.1	109	72.4	93.0	32.81	-119.70	63.99	850	2.6E+10	135.1	155.3	94/01/15 13:27:42	124.4	3.3	3.7	1
1994/01/15 15:23:29	T	99.4	191	78.7	99.3	32.84	-119.86	48.70	1025	1.5E+10	123.2	148.5	94/01/15 15:22:56	127.2	3.5	3.6	3
1994/01/15 16:42:57	T	99.4	168	80.4	99.3	32.83	-119.78	56.02	1150	2.0E+10	112.1	135.3	94/01/15 16:42:19	126.2	3.4	3.2	8
1994/01/15 16:52:12	T	85.9	31	71.8	85.8	32.80	-119.60	73.11	1325	3.4E+10	155.4	165.6	94/01/15 16:51:24	115.6	2.8	4.1	1
1994/01/15 17:10:48	T	101.5	125	82.5	101.4	32.84	-119.86	48.70	1025	1.5E+10	123.2	150.7	94/01/15 17:10:15	129.4	3.6	3.6	3
1994/01/15 17:22:00	T	92.7	43	73.7	92.6	32.90	-119.90	44.41	1075	1.3E+10	155.4	173.0	94/01/15 17:21:30	118.6	3.0	4.4	1
1994/01/15 17:30:57	T	97.2	184	76.2	97.1	32.84	-119.86	48.70	1025	1.5E+10	123.2	146.7	94/01/15 17:30:24	125.4	3.4	3.5	3
1994/01/15 19:07:50	T	97.8	118	76.8	97.7	32.94	-120.04	34.85	950	7.9E+9	99.2	122.3	94/01/15 19:07:27	122.1	3.2	3.7	10
1994/01/15 22:16:27	T	101.2	79	76.5	101.0	32.84	-119.86	48.70	1025	1.5E+10	123.2	150.3	94/01/15 22:15:54	128.9	3.6	3.6	3
1994/01/15 22:46:04	T	96.9	179	79.6	96.8	32.87	-119.78	55.21	1200	2.0E+10	112.2	135.1	94/01/15 22:45:27	125.8	3.4	3.2	8
1994/01/16 3:20:02	T	97.9	73	77.8	97.8	32.84	-119.86	48.70	1025	1.5E+10	123.2	144.8	94/01/16 03:19:29	123.5	3.3	3.5	3
1994/01/16 4:05:31	T	90.0	48	75.6	89.8	32.87	-119.85	48.92	1125	1.5E+10	133.3	146.2	94/01/16 04:04:58	114.8	2.7	3.5	2
Min		82.7	31.0	71.3	82.6	32.8	-120.1	25.5	775	4.3E+9	99.2	190.6		187.9	2.8	2.6	82.7
Max		101.1	254.0	82.5	101.0	32.9	-119.6	73.1	1325	3.4E+10	155.4	246.8		202.9	3.7	4.4	101.1
Avg		94.3	121.5	75.8	94.1	32.9	-119.9	48.0	1076	1.5E+10	124.7	218.9		195.7	3.3	3.5	94.3

INITIAL DISTRIBUTION

84310	Technical Library/Archives	(1)
71770	W. Teeter	(1)
75650	R. Wroblewski	(1)

Defense Technical Information Center
Fort Belvoir, VA 22060–6218 (1)

This page is intentionally blank.

REPORT DOCUMENTATION PAGE

Form Approved
OMB No. 0704-01-0188

PLEASE DO NOT RETURN YOUR FORM TO THE ABOVE ADDRESS.

1. REPORT DATE *(DD-MM-YYYY)*	2. REPORT TYPE	3. DATES COVERED *(From - To)*
January 2023	Final	

4. TITLE AND SUBTITLE

Ocean Acoustic Analysis of the 1994 Northridge Earthquake

5a. CONTRACT NUMBER

5b. GRANT NUMBER

5c. PROGRAM ELEMENT NUMBER

6. AUTHORS

Dr. Scott C. McGirr
Wayne L. Teeter
Dr. Ronald Wroblewski
NIWC Pacific

5d. PROJECT NUMBER

5e. TASK NUMBER

5f. WORK UNIT NUMBER

7. PERFORMING ORGANIZATION NAME(S) AND ADDRESS(ES)

NIWC Pacific
53560 Hull Street
San Diego, CA 92152–5001

8. PERFORMING ORGANIZATION REPORT NUMBER

TR-3303

9. SPONSORING/MONITORING AGENCY NAME(S) AND ADDRESS(ES)

10. SPONSOR/MONITOR'S ACRONYM(S)

11. SPONSOR/MONITOR'S REPORT NUMBER(S)

12. DISTRIBUTION/AVAILABILITY STATEMENT

DISTRIBUTION STATEMENT A: Approved for public release. Distribution is unlimited.

13. SUPPLEMENTARY NOTES

Author Scott McGirr is retired and no longer works at NIWC Pacific. Please contact Wayne Teeter for any questions on this report.

14. ABSTRACT

Ocean acoustic activity was analyzed before and after the 1994 Northridge earthquake. Hydrophones in the California Continental Borderland recorded primary waves (P-wave) and tertiary waves (T-wave) over an 80-hour period. Ocean-based acoustic data was analyzed and compared to concurrent land-based seismographic data. The P-waves detected correlated with the land seismic events. The T-waves detected did not correlate with seismic data. T-waves, localized by Line of Bearing (LOB) cross-fixing, were along the Ferrelo Fault zone in a major lateral offset. Land seismic sensors showed no precursors to the earthquake. Ocean acoustic sensors showed seaquakes occurring at a rate of 5.3/hour, which stopped 31 hours 20 minutes prior to the main earthquake and returned to near prior activity levels 16 hours later. Ocean quakes may indicate energy release during earth movement and its absence indicates energy accumulation as elastic strain in rocks. Hydrophones provide a valuable means to monitor geologic activity in borderland regions and can contribute to the understanding of coastal earthquakes.

15. SUBJECT TERMS

Earthquake, seaquake, data fusion, seismic acoustic, California Borderland

16. SECURITY CLASSIFICATION OF:			17. LIMITATION OF ABSTRACT	18. NUMBER OF PAGES	19a. NAME OF RESPONSIBLE PERSON
a. REPORT	b. ABSTRACT	c. THIS PAGE			Wayne Teeter
U	U	U	SAR	52	19B. TELEPHONE NUMBER *(Include area code)* (619) 553-2036

This page is intentionally blank.

This page is intentionally blank.

Naval Information Warfare Center (NIWC) Pacific
San Diego, CA 92152-5001